

LASER BEAM INTENSITY MEASUREMENT TO DERIVE ATMOSPHERIC PARAMETERS

A Project Report

Submitted By

CH. KAVYA SRI MEGHANA	2072050
T. LAKSHMI PRASANNA	2072059
D. MUKTHA SREE	2072074
N. NAVYA	2072080
A. POOJITHA	2072084

In partial fulfillment for the award of the degree of

BACHELOR OF TECHNOLOGY

IN

ELECTRONICS AND COMMUNICATION ENGINEERING

Under the guidance of

Dr. T. RAJENDRA PRASAD

(Scientist/Engineer-SF, NARL)

&

Mrs. T. NIRMALA, M.Tech., (Ph.D)

Assistant Professor (Senior)



ELECTRONICS AND COMMUNICATION ENGINEERING

SCHOOL OF ENGINEERING AND TECHNOLOGY

SRI PADMAVATI MAHILA VISVAVIDYALAYAM

(WOMEN'S UNIVERSITY)

TIRUPATI - 517502, A.P, INDIA

2020 - 2024



Department of Electronics and Communication Engineering

STUDENT DECLARATION

We hereby declare that the project entitled “**Laser Beam Intensity To Measure Atmospheric Parameters**” submitted by us to the Department of Electronics and Communication Engineering, School of Engineering and Technology, Sri Padmavati Mahila Visvavidyalayam, Tirupati in partial fulfillment of the requirements for the award of the degree of **Bachelor of Technology in Electronics and Communication Engineering** is a record of bonafide work carried out by us at NARL, under the supervision of **Dr. T. RAJENDRA PRASAD**, Scientist/Engineer-SF, NARL and **Mrs. T. NIRMALA, M.Tech., (Ph.D) Assistant Professor (Senior)**. We further declare that the work reported in this project has not been submitted and will not be submitted either in part or in full for the award of any other degree or diploma of this institute or of any other Institute or University.

Place: Tirupati

Signature of the Candidate

Date:

Ch. Kavya Sri Meghana	(2072050)
T. Lakshmi Prasanna	(2072059)
D. Muktha Sree	(2072074)
N. Navya	(2072080)
A. Poojitha	(2072084)



Department of Electronics and Communication Engineering

BONAFIDE CERTIFICATE

This is to certify that the project report entitled “**LASER BEAM INTENSITY MEASUREMENT TO DERIVE ATMOSPHERIC PARAMETERS**” submitted by **Ch. Kavya Sri Meghana, T. Lakshmi Prasanna, D. Muktha Sree, N. Navya, A. Poojitha** to School of Engineering and Technology, Sri Padmavati Mahila Visvavidyalayam, Tirupati in partial fulfillment of the requirement for the award of the degree of **B.Tech in Electronics and Communication Engineering** is a record of bonafide work carried out by them at NARL, under my guidance. The project fulfills the requirements as per the regulations of this University and in my opinion meets the necessary standards for submission. The contents of this report have not been submitted and will not be submitted either in part or in full, for the award of any other degree or diploma and the same is certified.

Guide :

Mrs.T.NIRMALA, M.Tech, (Ph.D).
Assistant Professor (Senior),
Department of ECE

Head of Department

Internal Examiner

External Examiner

ACKNOWLEDGEMENT

The satisfaction and elation that accompany the successful completion of any task would be incomplete without the mention of the people who have made it a possibility. It is a privilege to express our gratitude and respect to all those who have guided and inspired us during the project work.

We extend our sincere gratitude for the successful completion of our 4-month internship cum project from December 21st 2023 to April 21st 2024 at the **National Atmospheric Research Laboratory (NARL)**. We are immensely grateful to **Dr. Amit Kumar Patra, FNA, FASc**, the Director of NARL for granting us this invaluable opportunity to learn and grow under his esteemed leadership and guidance.

We would like to extend a special thanks to **Dr. T. K. Ramkumar** for selecting us and offering this internship opportunity at NARL. His confidence in our abilities and his support throughout the internship period have been instrumental in our professional development and learning experience.

We are deeply appreciative of **Dr. T. Rajendra Prasad** for his unparalleled mentorship, profound insights, and unwavering support throughout the project. His expertise in atmospheric science has been instrumental in shaping our research and enhancing our understanding of complex scientific concepts.

We extend our sincere thanks to **Dr K. Ragunath, Dr. Jyoti Bhate, A. Abhishek**, and **G. Sandeep** for their invaluable contributions and guidance, which have been crucial to the success of our project.

We would like to express our gratitude to the management of the CDMG, LAWP for providing us with excellent facilities and support, which greatly facilitated the execution of our project.

We would like to thank **Dr. T Narayana Rao** for his guidance, which was crucial in navigating the complexities of our project.

We are immensely thankful to all the individuals and entities at NARL who contributed to this enriching experience, which has been pivotal in our professional and academic growth.

We express a profound sense of gratitude and sincere thanks to our beloved Director, **Prof. V. Mallikarjuna**, for motivating us and providing the necessary permissions to carry out the project at NARL. We thank the Head of the Department (ECE), **B. Madhavi, M. Tech, (Ph. D)**, for her timely help and guidance whenever required.

We find immense pleasure in expressing profound gratitude and thanks to our Guide **Mrs. T. Nirmala, Assistant Professor (Sr.)**, Department of **Electronics and Communication Engineering** for standing by our side all through the project.

We thank all Department of ECE staff members for their support. We place on record special thanks to our parents and friends who were with us all through the course of our project.

Ch. Kavya Sri Meghana	(2072050)
T. Lakshmi Prasanna	(2072059)
D. Muktha Sree	(2072074)
N. Navya	(2072080)
A. Poojitha	(2072084)

LIST OF CONTENTS

CHAPTER NO:	TITLE	PAGE NO:
	Title page	i
	Declaration	ii
	Certificate	iii
	Acknowledgement	iv-v
	List of Contents	vi-vii
	List of Figures	viii-ix
	List of Tables	x
	Abstract	1-2
	Introduction	3-4
1.	Literature Survey	5- 18
1.1	Introduction	6-13
1.1.1	Refractive Index of Air	9-10
1.1.2	Refractive Index structure Parameter C_n^2	10-11
1.1.3	Atmospheric Optical Turbulence Model C_n^2	12-13
1.1.4	Effect of Dielectric Constant changes in Medium on EM wave propogation	13-14
1.2	NARL Expertise and Equipment related to Scintillometer	15-17
1.2.1	NARL AWS, Flux Towers	15
1.2.2	Atmospheric flux measurement equipment at NARL	15-17
1.3	History of Scintillometers development.	17-18
2.	Scintillometer	19-27
2.1	Introduction	19-20
2.1.1	Instrument Basics	20
2.2	Theory	21
2.2.1	Principle of Scintillometer	21

2.3	Types of Scintillometer	22
2.3.1	Optical Small Aperture Scintillometer	22
2.3.2	Optical Large Aperture Scintillometer	23
2.3.3	Laser Scintillometer	23-24
2.3.4	Microwave Scintillometer	24-25
2.4	Parameters Used	25
2.4.1	Intensity Fluctuations-The Variance	26
2.5	Scintillometer Equations	26-27
3.	Laser Scintillometer Experimentation	28-35
3.1	Introduction	29
3.1.1	Laser Properties	29
3.1.2	Principle of Laser	29
3.2	Classification of Laser by method of Generation	29-30
3.3	Applications of Laser	30
3.4	Selection of Modules for Instrumentation	30-35
3.4.1	Laser Source	31
3.4.1.1	Specifications of He-Ne laser	31-32
3.4.1.2	Advantages of Laser	32
3.4.2	Photo Detector	33
3.4.2.1	Specifications of Photo Detector	33
3.4.3	Oscilloscope	34
3.4.3.1	Specifications of Oscilloscope	35
4.	Methodology for Measuring Parameters	36-44
4.1	Process	37
4.2	Block Diagram	37
4.3	Laser Intensity Measurement Experiments	38-39
4.3.1	Laser Beam Propagation within Laser	39-40

	Lab between two labs	
4.3.2	Laser beam Propagation Outdoor Environment	41-42
4.3.3	Laser beam Propagation Building to Building	43-44
5.	Result	45-50
5.1	Room to Room Values at Room Temperature	46
5.2	Room to Room Values by Creating Turbulence	47
5.3	Outdoor Environment	47-48
5.4	Building to Building	48-50
6.	Conclusion & FutureScope	51-52
7.	Applications	53-55
8.	Bibliography	56-57

LIST OF FIGURES

FIGURE NO:	DESCRIPTION	PAGE NO:
1.1	Representation of eddies	6
1.2	Turbulence Spectrum	11
1.3	The 36-hour time series of scintillometer data compared to model output	13
1.4	a. Flux Towers(15m,50m) b. Humidity Sensor c. Rain Gauge	16
1.5	Microwave Radiometer	16
2.1	Schematic Representation of Scintillometer Principle	21
2.2	Optical Small Aperture Scintillometer(a&b)	22
2.3	Optical Large Aperture Scintillometer(a&b)	23
2.4	Laser Scintillometer	24
2.5	Microwave Scintillometer	25
2.6	Scintillation Spectra from Simultaneous LAS and MWS Measurements	26
3.1	Principle of Laser	29
3.2	He-Ne Laser	31
3.3	Internal Structure of He-Ne Laser	31
3.4	Photo Detector	33
3.5	Oscilloscope	34
4.1	Experimental Setup	38
4.2	Photo Detector	39
4.3	Oscilloscope	39
4.4	Mean and Standard Deviation Graphs for	40

	Room to Room at Room Temperature	
4.5	Mean and Standard Deviation Graphs for	
id41		
	Room to Room with Turbulence	
4.6	Experimental Setup from Hut to Hut	41
4.7	Mean and Standard Deviation Graphs for	42
	Outdoor Environment	
4.8	Laser Source in the Building	43
4.9	Landscape	43
4.10	Laser Beam Spot	43
4.11	Photo Detector in the Building	44
4.12	Mean and Standard Deviation graphs for	44
	Building to Building Readings	

LIST OF TABLES

FIGURE NO :	DESCRIPTION	PAGE NO
2.1	Types of Scintillometer-Measured variables	25
4.1	Overview of Calculations	38
5.1	Room to Room (at Room Temperature)	46
5.2	Room to Room (with some Turbulence)	47
5.3	Hut to Hut	47-48
5.4	Building to Building	48-50

ABSTRACT

The project's objective is to develop a Laser Scintillometer. The laser beam Intensity fluctuation caused by atmospheric parameters is measured using a laser source and photodetector setup. Selection of laser source, photo detector and data acquisition system is performed. An optimal 1-mm diameter, 633 nm wavelength laser beam with 1-mW stabilized energy level laser Source is selected from the available calibration / alignment lasers of High Energy Laser Lab. A Photodetector with optimal spectral range with a diffuser is selected from the energy meters, to convert laser light to electrical signal at the receiver end for the scintillometer experiment. An oscilloscope based data acquisition system is envisaged to collect digital data, instead of developing a dedicated ADC and data acquisition system, for simplicity. The Oscilloscope is set to sample the input voltage from photodetector at 10 HZ, by generating 1000-point data series in 90 sec duration in each data file to match the high speed atmospheric flux measurement equipment.

A number of sets of experiments are conducted in the laboratory, in real atmospheric conditions with different turbulence levels. The first measurements with this test setup are on the optical bench, to receive the laser beam at 1m distance. With satisfactory data collection on the optical bench, the laser beam propagation distance is increased from 1 m to 3.5 m within the two rooms of the laser lab. In the next step, artificial turbulence is introduced by creating air movement thus turbulence and temperature changes in the lab. The data is analyzed and found to have more variance compared to the previous experiment, due to the turbulence. The experimental setup is shifted to the outdoor environment with the laser beam propagation path of 20 m distance, at 2 m height near the flux towers, with an intention of validating the derived parameters with flux towers data. This attempt has limited success because the sensitive lab based photodetector is being used in bright sunlight and excessive temperature of the outdoor environment even at 3:30 PM to 5 PM time period.

To overcome the limitations, in this final experimental setup, the Laser source is kept in the first building and the receiving photodetector and oscilloscope data acquisition setup is placed in the other lab with a controlled environment. The Laser beam is pointed through small window openings of one building to another building. The Laser beam is propagating to a distance of 60 m over at a height of about 5 m in this setup, passing over a natural terrain of green lawn grass, bitumen road and stones. The data collection is performed at around 12:30 pm to 3:30 pm duration, where the turbulence is expected to be maximum.

The collected data enabled us to discern the impact of atmospheric turbulence on laser propagation. The laser beam intensity variance parameter is meticulously measured and analyzed. The derived atmospheric parameters include temperature heat flux and turbulence-based scintillations from the variance in the 1000-point data series due to the fluctuations in air refractive index forming eddies in the laser beam

propagation path. By establishing a clear link between laser beam intensity variance/standard deviation and atmospheric conditions, our project contributed to atmospheric studies and practical applications, to be used in precision agriculture for the effective utilization of water resources.

Statistical analysis, focusing on mean and standard deviation forms the cornerstone of our analytical approach, guiding us in deriving crucial atmospheric parameters temperature/heat flux, turbulence and air refractive index structure constant. Understanding and quantifying these parameters is crucial for applications ranging from environmental monitoring, strategic defense applications to optical communication.

INTRODUCTION

This research project is dedicated to the development of laser scintillometers with the overarching goal of deriving essential atmospheric parameters. Atmospheric conditions, characterized by turbulence and thus varying refractive indices, exert significant influence on the propagation of laser beams, impacting various applications from environmental monitoring, strategic defense applications to free-space optical communication. The primary focus of this project is the experimentation of a Laser Scintillometer, a sophisticated instrument designed to measure laser beam intensity fluctuations caused by atmospheric factors. By employing state-of-the-art optical sensors and advanced data analysis techniques, the research project aims to capture the intricate variations in laser beam intensity induced by atmospheric turbulence and refractive index fluctuations.

Controlled experiments are conducted in both laboratory and real atmospheric conditions with varying turbulence levels. The experimental setup involves a laser source and photodetector arrangement, enabling the collection of data at a rate of approximately 10 Hz in 90-second intervals. This data collection allows for the measurement and analysis of laser beam intensity variance parameters, providing insights into the influence of atmospheric turbulence on laser propagation.

Through meticulous measurement and analysis of laser beam intensity fluctuations under varying atmospheric conditions, the research aims to elucidate the complex dynamics of the atmosphere. In conclusion, this research project represents a concerted effort to enhance our ability to measure and understand atmospheric parameters through precise laser beam intensity measurement.

Chapter 1 of this project report presents the literature survey, the simplified understanding of complex dynamics and thermodynamics in the atmosphere near to the earth surface. The formation of eddies, the transfer of heat from land to air, and flux of physical parameters from one air parcel to another parcel, heat and momentum flux are briefed. The flux of these atmospheric parameters create turbulence in the air movement, and rapid variations of parameters create rapid changes in the refractive index, thus these create scintillations, which change the path and delay time of electromagnetic wave propagation. This chapter also presented the expertise and equipment available at NARL in dealing with Radars with atmospheric air refractive index as target, LIDARs which use EM radiation sources in Optical, Infrared and UV spectrum. The atmospheric boundary layer meteorological research equipment and research activities at NARL are presented, which are crucial to the aim of the project. The Scintillometer Instrument development history details are presented as this technique development took a few decades due to the complexities of optical, laser

and microwave (160 GHz) signal generation processing advancements with Indian and foreign researchers' context.

Chapter 2 presented the Scintillometer background theory, different types of scintillometers development, such as Optical small aperture, Optical large aperture, Laser based, Microwave based scintillometers and the measured parameters. The optical and laser Scintillometers derive heat flux, as this wavelength is best suited to temperature parameters. The microwave scintillometer is applicable for humidity flux determination. Combined together gives further information of the atmospheric covariance parameters. The Dual beam Scintillometer provides wind velocity parameters as per the literature. The availability of commercial scintillometers is presented in the chapter.

Chapter 3 is dedicated to the instrumentation selection for the Scintillometer experimentation. The fundamentals of Laser, classification of lasers based on generation, applications of Lasers, selection of available instruments like calibration laser source, precision lab based photodetector and data acquisition methodology using sophisticated modern digital oscilloscope are discussed. The digital data is stored on the USB drive for further processing in a digital computer.

Chapter 4 is on the step by step experimentation of Scintillometer. The data collection procedure, experimental setup updates and obtained data series and estimated parameter of C_n^2 values are presented.

Chapter 5 presented the results of the data processing. The measured values are near the range of the theoretical refractive index structure constant C_n^2 .

Chapter 6 stated the conclusion and future scope of the 'Laser Beam Intensity Measurement To Derive Atmospheric Parameters' activity. The limitation of this simplified scintillometer is understood as the receive aperture of the photodetector is smaller than the laser beam aperture, after the beam propagation of 60-m in the receiver lab, where photodetector and oscilloscope DAQ are present. This limitation can be overcome by appropriate optics both at transmit and receive end of the test set up, in the future development activities. The commercial scintillometer is envisaged and low cost modules are being explored to develop scintillometers for about 100-500 meter range of field, where the majority agriculture fields in India are within this range.

Chapter 7 presented the advantages of Scintillometers in agriculture to remote sensing and military applications.

CHAPTER -1

LITERATURE SURVEY

1.1 INTRODUCTION

Our planet Earth is a highly complex system formed by mutually coupled components (land, atmosphere and ocean) and processes and exchanges that occur over a wide range of temporal and spatial scales. The land-atmosphere interface, the surface boundary layer of the Earth within 50 m height is particularly crucial for the functioning of the Earth system through interactions via mass, energy and momentum fluxes as well as through biogeochemical cycles.

The exchanges of momentum, heat and moisture at the surface between the atmosphere and the underlying earth's surface strongly influence in many ways the dynamics and thermodynamics of the atmospheric system. The dynamics of the atmosphere are mainly by airflow. The airflow in the atmosphere can be imagined as a horizontal flow of numerous rotating eddies. Each eddy has 3-D components including vertical movement of the air. The physical mechanisms involved in the generation of eddies in a typical airflow and the creation of turbulence is pictorially represented in Figure 1.1.

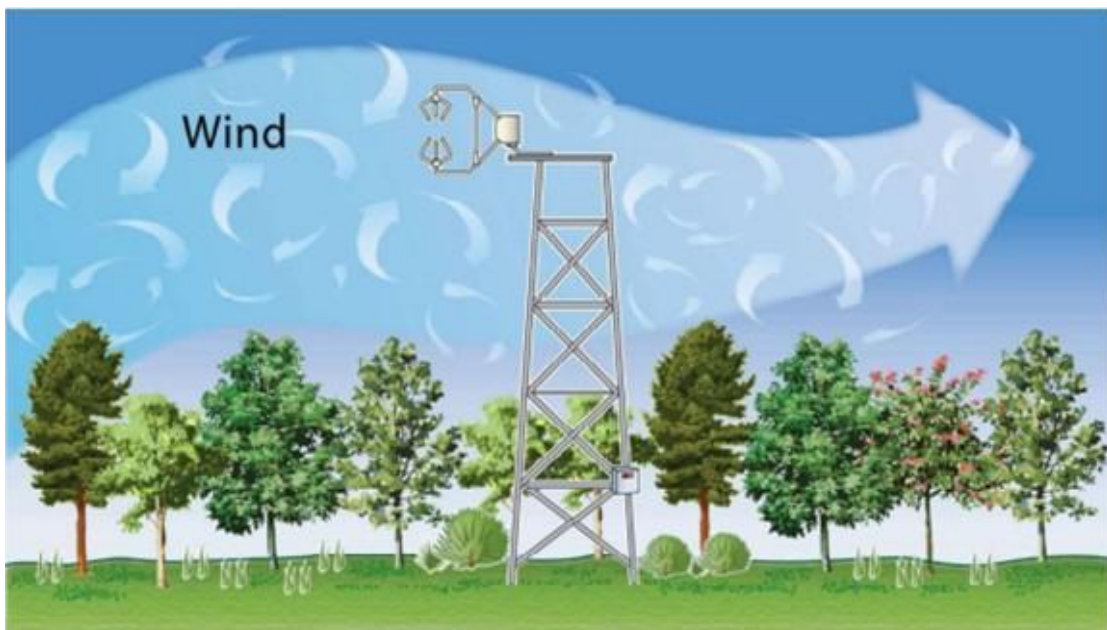


FIGURE 1.1 Representation of eddies and the flux of parameters in air flow

Closer to the ground, there is a stronger probability of smaller eddies rotating fast and being responsible for the transport of most of the flux by higher frequency movements. Larger eddies rotate slowly and are responsible for the transport of most of the flux by lower frequency movements. In practical terms, there is always a mix of different eddy sizes.

Earth's radiation budget deals with the energy component received from the sun and that radiates back to space. Absorbed radiation increases the temperature. Emitted radiation lowers the temperature and the radiation budget is said to be in balance if both are equal. The exchange of heat occurs when the temperature of the air is different from that of the surface. Depending on whether the surface is warmer or cooler than the air next to it, heat is transferred to or from the atmosphere by turbulent air motion. This effect also increases with increasing temperature difference and increasing surface wind speed. Such warming and cooling are sensitive to wind speed.

The heat flux is defined as the amount of heat per unit time passing through the unit area. The majority of the available energy at the surface is used in Evapotranspiration (ET) processes rather than heating the surface. The latent heat is transferred to the atmosphere, it is released when water vapor condenses and changes back from vapor to liquid. The release of this heat provides energy that fuels storms and atmospheric circulation. These transitions near the surface and lower atmosphere dictate the local weather phenomena like thunderstorm events which are highly dependent on topography, vegetation, soils, landforms and structures. The Surface Energy Balance (SEB) is an important boundary condition for the land surface, determining the partitioning of the available energy. The radiation components and surface energy distribution are controlled by characteristic surface factors such as vegetation cover and roughness length and subsequently affect micrometeorological elements such as temperature, humidity, and precipitation.

The estimation of atmospheric turbulent fluxes at the land surface has been recognized as the most important process in the determination of the exchanges of energy and mass among hydrosphere, atmosphere and biosphere. Flux is calculated as a covariance of instantaneous deviations in either heat or moisture.

The turbulent fluctuations of heat or moisture must be measured at a high sampling frequency (10-20 Hz). The measuring or sampling time depends on the atmospheric stratification, the wind velocity, and the measuring height. The turbulence measurement is attracting increasing attention from the scientific society of hydrology, atmosphere, environment, remote sensing, and ecology. Agricultural meteorology and hydrology are concerned with the intensity of turbulence and the energy balance at the surface.

Statistical methods are used (agricultural sciences, etc.) to determine exchange rates over natural ecosystems and agricultural fields and to quantify, estimate momentum, heat, water vapor fluxes. These fluxes are used extensively for the verification and tuning of global climate models, weather models, and remote sensing estimates from satellites and aircraft. The technique is mathematically complex and requires significant care in setting up and processing data. To date, there is no uniform terminology or a single methodology, but much effort is being made by

flux measurement networks like FluxNet, Ameriflux, ICOS, CarboEurope, Fluxnet Canada, OzFlux, NEON, and iLEAPS.

The 3D wind or temperature are decomposed into mean and fluctuating components. In mathematical terms, "eddy flux" is computed as a covariance between instantaneous deviations in vertical wind speed from the mean value. Several mathematical operations and assumptions, including Reynolds decomposition, are involved in getting from physically complete equations of the turbulent flow to practical equations for computing "eddy flux". Measurements at a point can represent an upwind. Flux is fully turbulent, most of the net vertical transfers are by eddies. If the terrain is horizontal and uniform, the average of fluctuations is zero, density fluctuations are negligible. Flow convergence & divergence are negligible.

Evapotranspiration (ET) is a part of the water cycle, and accurate ET readings are important to local and global models to manage water resources. ET rates are an important part of research in hydrology-related fields, as well as for farming practices. Micrometeorology focuses climate study on the specific vegetation canopy scale. The effect of turbulence is of specific interest to climate modelers or those studying the local ecosystem.

Wind speed, turbulence, and mass (heat) concentration are values that could be recorded in a flux tower. Wetland vegetation varies widely and varies from plant to plant ecologically. Readings can be taken from flux towers over several years to determine water use efficiency among others. By measuring the vertical turbulent flux of gas states of H_2O , CO_2 , heat, and CH_4 monitoring equipment can be used to infer canopy interaction. Vegetation production models require accurate ground observations, in this context from eddy covariance flux measurement.

Instruments can detect very small changes at high frequencies, ranging from a minimum of 5 Hz to 40 Hz using tower-based measurements. Common uses are Greenhouse gas emissions, Measuring water loss, evapotranspiration, Instantaneous water use efficiency, and Instantaneous radiation use efficiency. The Novel uses are Precision Irrigation, and Precision Agriculture.

The fast temperature and moisture variations create density fluctuations in the air called turbulence, which in turn alter the refractive index of air. Hence, the heat or moisture flux can be measured using the changes in the refractive index of air. The refractive index of air at standard conditions often denoted as n_0 , is approximately 1.00028. The refractive index is related to temperature, humidity and pressure as per the equation presented in the next section.

The air refractive index changes in the order of the fourth decimal point, due to changes in the physical parameters. The propagation of electromagnetic waves is affected by these small air dielectric constant changes. Light being electromagnetic energy, the propagation of light and the effects of turbulence on light propagation are

basic methodology of Scintillometer, Laser Scintillometer development is experimented to derive the turbulence and there by heat flux measurement to get precise time of watering the agriculture fields.

1.1.1 REFRACTIVE INDEX OF AIR

Electromagnetic signal propagation is affected with variation in radio refractive index of the atmosphere which in turn depends on variability of humidity, temperature and electron density induced by turbulence in the atmosphere.

For an atmospheric radar, the mean received echo power due to volume scatter is given by

$$P_r \propto \frac{P_t A_e \eta r}{4\pi R^2}, \quad \text{-----> Eq1.1}$$

Where,

P_t = Transmitter power

A_e = Effective antenna area

r = Range resolution

R = Range of reflecting volume

η = Volume reflectivity coefficient

The value of Volume Reflectivity Constant “ η ” is a function of turbulence in the atmospheric air motion, Where,

$$\eta = 0.38 C_n^2 \lambda^{-1/3} \quad \text{-----> Eq1.2}$$

where,

C_n^2 = Refractive index structure constant

λ = Operating wavelength

$$C_n^2 = a \langle n^2 \rangle L_a^{-2/3} \quad \text{-----> Eq1.3}$$

where,

C_n^2 = Refractive index structure constant

$\langle n^2 \rangle$ = mean square fluctuation of ‘n’ the refractive index

$L_a^{-2/3}$ = Outer scale of turbulence in inertial sub range (a function of turbulent energy dissipation rate and buoyancy frequency), and

“a” is the proportionality constant.

Where,

Refractive index is related to temperature, pressure and humidity (water vapor) as follows.

$$n = 1 + 77.6 \times 10^{-6} \rho / T \text{ (Dry Term)} + 3.73 \times 10^{-1} e / T^2 \text{ (Wet Term)} - 40.3 N_e / f_o^2 \quad \text{-----> Eq1.4}$$

where,

n = Refractive index

e = Partial pressure of water vapor (in Mb)

ρ = Atmospheric pressure (Mb)

T = Absolute temperature

N_e = No. density of free electrons (at ionosphere height region) per m^3

f_o = Operating frequency in Hz

The fast changes of temperature and humidity create atmospheric turbulence and alter the refractive index of air; fluctuations of air dielectric constant results in variations of propagation speed and direction parameters of EM waves.

1.1.2 REFRACTIVE INDEX STRUCTURE PARAMETER C_n^2

C_n^2 refers to the refractive index structure parameter. It is a measure of the strength of turbulence in the atmosphere. It represents the spatial and temporal variations in the refractive index of air. The notation C_n^2 stands for the "structure parameter of the refractive index of air." It quantifies the strength of atmospheric turbulence in terms of how much the refractive index of air fluctuates over a given distance. It is defined as the spatial average of the refractive index fluctuations squared per unit length.

The propagation of electromagnetic waves, such as light or radio waves is impacted by atmospheric turbulence. Measurements or estimations of C_n^2 are essential for predicting and mitigating the effects of atmospheric turbulence. It is often used in the context of atmospheric turbulence to quantify the strength of turbulence or the "turbulence intensity."

It is defined as the variance of the refractive index fluctuations per unit length. When it is large, it indicates strong turbulence, which can significantly affect the propagation of light through the atmosphere, causing effects such as scintillation, beam spreading, and image distortion. Conversely, when it is small, the atmosphere is considered to be relatively calm with minimal turbulence effects. The specific value of C_n^2 depends on various factors such as altitude, time of day, and atmospheric conditions.

C_n^2 is calculated using measurements of atmospheric turbulence, often obtained through instruments like scintillometers, representing the spatial variation of refractive index in the atmosphere. C_n^2 describes the fluctuations in the refractive index of air as a function of distance. "Cn squared" (often denoted as C_n^2) refers to the refractive index structure parameter in atmospheric optics and turbulence studies.

The refractive index of air at standard conditions provides a baseline reference for comparison, while C_n^2 quantifies the turbulent fluctuations in the refractive index that affect light propagation through the atmosphere. In atmospheric optics and related

fields, the structure parameter of refractive index fluctuations is often measured in units of meters to the power of $-2/3$ ($\text{m}^{-2/3}$). This unit might seem unusual, but it's a convention chosen for convenience and to reflect the behavior of turbulence in the atmosphere. The power of $-2/3$ is derived from the Kolmogorov turbulence theory, which describes the behavior of turbulence in a fluid medium [2]. According to this theory, in the inertial subrange of turbulence (where energy is transferred from large scales to small scales), the spectrum of refractive index fluctuations scales with a power of $-5/3$. Integrating this spectrum over spatial frequencies yields a structure parameter with units of length raised to the power of $2/3$ ($\text{m}^{2/3}$). To simplify the representation and to align with common atmospheric turbulence conventions, this length scale is often expressed as a negative exponent, resulting in units of $\text{m}^{-2/3}$.

This representation makes the parameter more intuitive in the context of atmospheric turbulence and its effects on optical propagation. So, when we say C_n^2 is measured in units of meters to the power of $-2/3$, it reflects the scaling behavior of turbulence and its influence on the refractive index fluctuations in the atmosphere

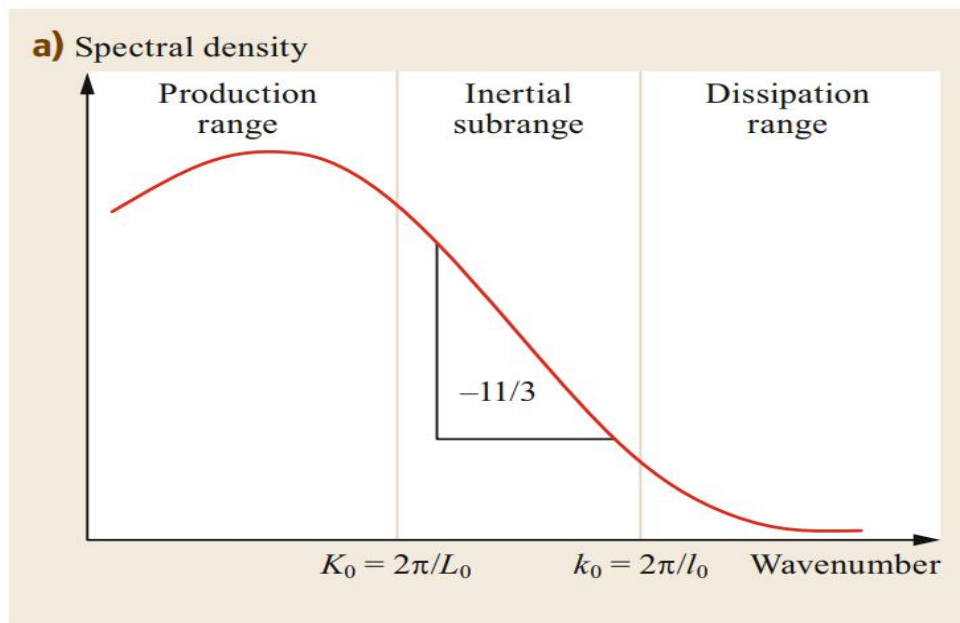


FIGURE 1.2: Turbulence Spectrum

The production range is where turbulent energy is generated by buoyancy and shear. The inertial subrange over which the energy is transferred from larger to smaller eddies. The dissipation range is where turbulent energy is dissipated into heat. Kolmogorov provided a model for the three-dimensional refractive index spectrum for homogeneous and isotropic turbulence in the inertial sub range.

1.1.3: THE ATMOSPHERIC OPTICAL TURBULENCE:

Atmospheric optical turbulence is a problem for most electro-optical (EO) systems in astronomy. The image distortion can drastically reduce system and sensor performance. A means of assessing the levels of optical turbulence, relying on calculations that require a minimum of atmospheric data.

The propagation of a light beam through the atmosphere is affected by random fluctuations in the refractive index of air. These fluctuations or discontinuities cause optical turbulence—variations in the speed at which the wavefront propagates. The refractive index structure parameter (C_n^2) is a quantitative measure of optical turbulence.

The value of C_n^2 has been generally observed to range from about 10^{-12} to $10^{-16} \text{ m}^{-2/3}$. High values of C_n^2 , $10^{-12} \text{ m}^{-2/3}$ or greater, even over nominal distances, usually indicate turbulent atmospheres wherein considerable visual blurring or image distortion would be present (as if one were looking out over a hot paved road, over an airport runway, or, in an extreme case, through the exhaust behind a jet engine). At lower values of C_n^2 , 10^{-16} to $10^{-15} \text{ m}^{-2/3}$, atmospheric optical turbulence would generally be considered negligible.

The C_n^2 reported on a refractive index structure parameter model makes a quantitative assessment of atmospheric optical turbulence given two levels of wind, temperature, and humidity profile data as input. That makes estimates of C_n^2 obtainable for unstable, stable, and near-neutral atmospheric conditions. C_n^2 also computes the surface heat and moisture flux.

Mathematical Description of C_n^2

The motivation for these studies was principally to develop and verify a set of equations for the atmospheric stability portion of the calculations needed to evaluate an expression for C_n^2 , such as the one given in Tatarski (1961), which can be written as

$$C_n^2(z) = b \frac{K_H}{\epsilon^{1/3}} \left(\frac{\partial n}{\partial z} \right)^2 \quad \text{-----> Eq1.5}$$

where b is equal to 3.2 and called the Obukhov-Corrsin constant, K_H is the turbulent exchange coefficient for heat diffusion, ϵ is the energy dissipation rate and $\frac{\partial n}{\partial z}$ is the vertical gradient of the index of refraction n .

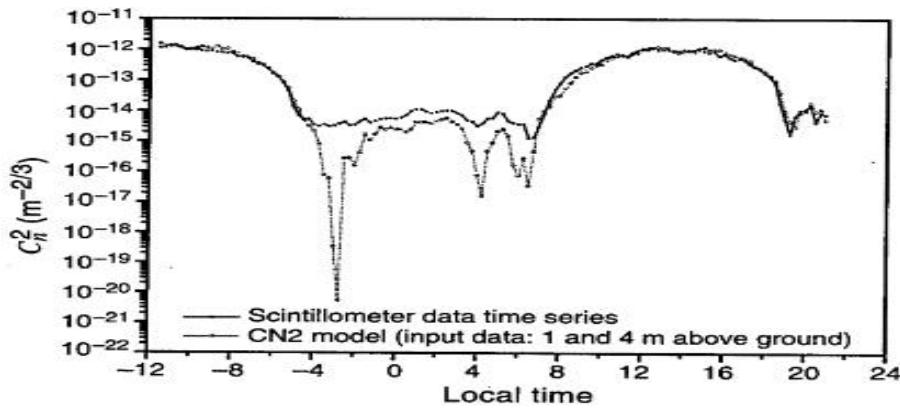


FIGURE 1.3: The 36-hour time series of scintillometer data compared to model output

Figure 1.3 presents a 36-hour variation Cn^2 in the scintillometer measurements compared with model data through the meteorological profiles. The micro meteorological profiles of wind speed, temperature, and relative humidity were measured on an 8-m tower centered in the test area (at 0.5, 1., 2., 4., and 8. m above the surface). The 0.94- μ m scintillometer was 2 m above ground over a path of approximately 450 m.

1.1.4 EFFECT OF DIELECTRIC CONSTANT CHANGES IN MEDIUM ON EM WAVE PROPAGATION

When the refractive index or dielectric constant of a medium rapidly changes, it introduces spatial gradients in the medium that can significantly affect electromagnetic (EM) wave propagation. Maxwell's equations govern how electric and magnetic fields interact with each other and with sources of charge and current in space. When dealing with linear, isotropic, and homogeneous media (where the refractive index and dielectric constant are constant), Maxwell's equations are simplified. However, when refractive index or dielectric constant rapidly change with space, these equations become more complex and often require numerical techniques for solution.

The effects of rapid changes in refractive index or dielectric constant on EM wave propagation are as follows.

1. Wavefront Distortion: Rapid changes in refractive index or dielectric constant can cause distortion of the wavefronts, leading to phenomena like scattering, diffraction, and aberrations.
2. Wave Dispersion: Dispersion occurs when different frequencies of the EM wave travel at different speeds in the medium. Rapid changes in refractive

index or dielectric constant can lead to significant dispersion effects, causing spreading of the pulse in time and frequency domains.

3. Reflection and Refraction: At boundaries where the refractive index or dielectric constant changes abruptly, reflection and refraction occur. The Fresnel equations describe how much of the incident wave is reflected and refracted at an interface with a different medium.

$$\nabla^2 E - \mu\epsilon \frac{\partial^2 E}{\partial t^2} = \mu\epsilon \frac{\partial^2 E}{\partial t^2} \text{-----> Eq1.6}$$

The wave equation analyzes these effects mathematically, which describes how the electric and magnetic fields propagate through space. The general form of the wave equation in a homogeneous, isotropic, linear, and non-conducting medium can be modified to account for spatially varying refractive index or dielectric constant by including spatial derivatives of the refractive index or dielectric constant. Solving this modified wave equation helps understand how rapid changes in these properties affect EM wave propagation.

1.2 NARL EXPERTISE AND EQUIPMENT RELATED TO SCINTILLOMETER

National Atmospheric Research Laboratory (NARL) is engaged in fundamental and applied research in the field of Atmospheric Sciences. The research institute was started in 1992 with MST Radar, and over the years, many facilities such as Mie/Rayleigh Lidar, Lower atmospheric wind profiler (LAWP), High-performance computers, and x-band weather radar were added.

The Advanced Indian MST Radar is used for atmospheric probing of the Mesosphere, lower Stratosphere, Troposphere and Ionosphere. This radar operates at 53 MHz, capable of providing estimates of atmospheric dynamics up to 25 km, with the radar target being the air, using the fluctuations in refractive index of air as target.

The Rayleigh Doppler Lidar (RDL) measures stratospheric and lower mesospheric mean winds using the electromagnetic radiation at 532 nm, using a steerable laser beam. A pulsed monostatic lidar system studies the atmospheric aerosols up to 30 km and the temperature up to 90 km height, both Lidars use 500 mJ high energy Laser Sources. The Boundary Layer Lidars are micro pulse low energy lidars developed for different applications in NARL. An imported micropulse lidar and Cieloment are operational round the clock to study boundary layer aerosol and cloud base studies. All these laser based instruments are providing the basic technology of low energy Transmitting Receiving modules of the Laser Scintillometer.

A multi-wavelength airglow photometer measures mesospheric OH emission levels from ~85 km at 840 nm and 846 nm, O₂ from 94 km at 866 nm and 868 nm, and thermosphere O (1D) from 220 km at 630 nm emission intensities with the help

of seven temperature-controlled interference filters having FWHM ~ 0.45 nm. These study the role of vertically propagating waves in the dynamics and energetics of the middle atmosphere using the optical instruments. The photometers and lidar systems receiving sections convert optical signals to electrical signals thus cater the receiving part of the Scintillometer.

The 15-m, 50-m flux tower, balloon launch facilities, LAWP, Rain Gauge Network, GNSS receivers, and X-band radar and Ku band receiving beacon system provide meteorological studies. The high-performance computer is used for the weather forecast utilizing satellite data. The trace gas, aerosol and radiation and atmospheric chemistry study provide another dimension of pollution and climate variations. The site is used to validate the atmospheric parameters retrieved from the satellites. The flux measurement by the flux towers provide an opportunity to compare the and validate the data of the scintillometer under development.

Since NARL has the expertise in Lasers, Radars with refractive index as target, ground based equipment like flux towers to estimate the heat fluxes, The new development of Laser Scintillometer is taken up. Experiments are conducted to study the effect of temperature fluctuations that cause turbulence in air and thus affect the propagation of laser beams. The laser beam intensity fluctuations are measured to estimate the air refractive index fluctuations C_n^2 and thus estimation of heat flux is taken up as the challenge of the project, which can be validated using the available equipment.

1.2.1. NARL AWS, FLUX TOWERS

NARL automatic weather station (AWS) measure basic meteorological parameters with sensors mounted on mast. AWS have a Thermometer for measuring temperature, Anemometer for measuring wind speed, Wind vane for measuring wind direction, Hygrometer for measuring humidity, Barometer for measuring atmospheric pressure, Ceilometer for measuring cloud height, Rain gauge for measuring liquid-equivalent precipitation, Pyranometer for measuring solar radiation.

NARL Flux towers are advanced systems with high speed sonic anemometers to measure vertical turbulent fluxes in atmospheric wind, energy, and momentum.

1.2.2. ATMOSPHERIC FLUX MEASUREMENT EQUIPMENT AT NARL

NARL flux tower, also known as an eddy covariance tower or micrometeorological tower, is a tall 15-meter structure equipped with instruments designed to measure the exchange of gas, heat, and momentum flux between the Earth's surface and the atmosphere.



FIGURE 1.4 : (a) Flux towers (15m, 50m) with sonic anemometers at top of the mast, (b) Humidity Sensor (c) Rain Gauge.



FIGURE 1.5: Microwave Radiometer

Flux towers are typically advanced high-speed parameter measurement instrumented towers with sensors at multiple levels. These measure a variety of atmospheric parameters, including humidity, temperature, and wind speed. The 50-meter high flux tower consists of sensors at 1, 2, 4, 8, 16 32, and 50-meter heights. GNSS receivers are installed at the site to get meteorological parameters.

A microwave radiometer is used to estimate water vapor and temperature profiles, derived from detecting the natural microwave radiation emitted by molecules in the Earth's atmosphere. They measure the intensity of microwave radiation at specific frequencies emitted by water vapor and oxygen. They can provide vertical profiles of water vapor concentration, temperature which is crucial for understanding humidity distribution in the atmosphere.

The Scintillometer directly measures turbulent fluctuations of the refractive index of air caused by variations in temperature, humidity, and pressure. It consists of an optical or/and radio wave transmitter, emitting em waves parallel to the earth's surface, and a receiver at the opposite end of the atmospheric propagation path, separated by 100m to 10000m. The development of the scintillometer is taken up based on the experimentation of the current project at NARL, with available low

power laser instruments, capability to validate the derived parameters with flux tower data.

1.3. HISTORY OF SCINTILLOMETER

Scintillometer is a relatively young discipline in atmospheric science and measurement technology [2]. The first systematic studies of scintillations were performed in the middle of the twentieth century by astronomers, and by engineers and scientists dealing with communication systems (on both ground-based and satellite platforms) and for military purposes (related to the development of laser defense systems).

After the theoretical description of wave propagation in a turbulent fluid and a theory to describe surface layer turbulence based on scaling arguments had been worked out in the 1950s and 1960s by Monin, Obukhov, and Tatarski, it was recognized that parameters characterizing atmospheric turbulent flows, notably, the dissipation rate of turbulent kinetic energy and the structure parameter of the refractive index (C_n^2) can be obtained from scintillation measurements wherefrom the vertical surface fluxes of momentum, sensible and latent heat can be derived.

First prototype research scintillometer systems were built and tested in the 1970s and 1980s by Wang, Hill, Ochs, and Frehlich. These systems were employed to further develop and verify the theoretical concepts and to demonstrate possible applications. However, most of these basic studies found little attention in the meteorological community. In the 1980s Kohsiek brought the design idea of a large-aperture scintillometer (LAS) to Europe. Subsequently, he built the prototype in 1991 to determine the sensible heat flux of a sparse vineyard, a strongly heterogeneous surface at a meter scale. The scintillometer fluxes were shown to compare very well with independent eddy-covariance measurements. This success initiated a very intense and fruitful period of scintillometer development and applications.

In the second half of the 1990s, the potential of the method and the robustness of the instruments were demonstrated under different climate and surface conditions and for a wide range of applications in meteorology, ecology, hydrology, and agriculture. A scintillometer setup in Germany was operational for about 20 years. Important theoretical developments are performed to qualify the scintillometer method and to define algorithms for data analysis and quality assurance/quality control. This contributed significantly to the design and realization of the commercial scintillometers.

About 10 years later multiple-LED LAS, called boundary-layer scintillometer (BLS) was developed. In the early 1980s, Kohsiek and Herben had shown that evaporation can be estimated from a combination of an optical LAS and a microwave

scintillometer (MWS) and later the MWS became commercially available. Scintillometers are currently in wide use for a variety of applications.

In India, Researchers from Indian Institute of Tropical Meteorology (IITM), Pune worked on development of Scintillometer during 1990s.[3]

CHAPTER -2

SCINTILLOMETER

2.1. INTRODUCTION

The human eye can see the twinkling of stars at night, and the distortion of the background over strongly heated surfaces during day time. The Light passing through the air parcels of varying refractive index leads to intensity fluctuations of the light at the eye. This phenomenon is called scintillation. Twinkling, also called scintillation, is a generic term for variations in apparent brightness, color, or position of a distant luminous object viewed through a medium. In simple terms, the twinkling of stars is caused by the passing of light through different layers of a turbulent atmosphere. Most scintillation effects are caused by anomalous atmospheric refraction caused by small-scale fluctuations in air density usually related to temperature gradients. Stars twinkle because they are so far from Earth that they appear as point sources of light, easily disturbed by Earth's atmospheric turbulence, which acts like lenses and prisms diverting the light's path. Twinkling usually does not cause images of planets to flicker appreciably. With multiple observed points of light traversing the atmosphere, their light's deviations average out and the viewer perceives less variation in the light coming from them.

The receiver detects and evaluates the intensity fluctuations of the transmitted signal, caused by refractive index variations. Scintillometers consist of a transmitter-receiver pair for electromagnetic radiation separated from each other by a distance of 10^2 - 10^4 m. As the emitted radiation travels through the atmosphere, it is affected by turbulent eddies of different densities. At the receiver, the resulting high-frequency intensity fluctuations of the electromagnetic signal (scintillations) are recorded, from which the turbulent sensible and latent heat fluxes can be derived. The signal at the receiver represents an integrated effect of the conditions along the path; scintillometers, therefore, provide area-averaged values of fluxes. This is of special relevance for applications like the validation of flux data from numerical weather prediction and climate models or satellite retrievals, or for the estimation of regional scale evaporation rates in agricultural management and hydrology. For example, the Scintillometer is very useful in the precise watering of agricultural fields.

2.1.1. INSTRUMENT BASICS

- Scintillometers consist of a transmitter-receiver pair of em wave radiation,
- As the emitted radiation travels through the atmosphere, it is scattered by turbulent eddies of different densities.

- At the receiver, the resulting high-frequency intensity fluctuations of the electromagnetic signal (scintillations) are recorded, from which the turbulent sensible and latent heat fluxes can be derived.

2.2. THEORY

Scintillometer relies on the theory of electromagnetic wave propagation in the turbulent atmosphere, relating the measured intensity fluctuations of an electromagnetic signal to the characteristics of atmospheric turbulence, quantified by the structure parameters of refractive index, temperature, and humidity. These are used to derive the surface fluxes of momentum, sensible and latent heat. This implies a series of assumptions, such as weak scattering of the emitted light beam, sensitivity to frequencies in the inertial subrange of turbulence, homogeneous and locally isotropic turbulence, and homogeneous surface and stationary atmospheric conditions.

2.2.1. PRINCIPLE OF SCINTILLOMETER

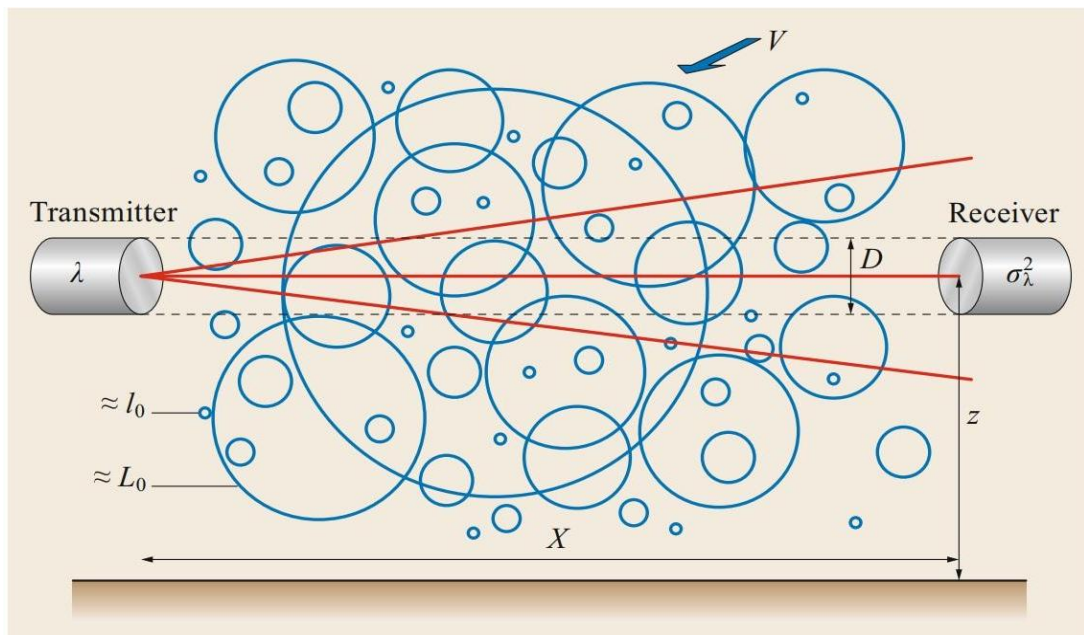


FIGURE 2.1 Schematic Representation of Scintillometer Principle

The principle of the scintillometer is illustrated in Fig 2.1. Electromagnetic radiation of wavelength is emitted at the transmitter with constant strength and propagates over a distance X towards the receiver where the time series of its intensity (i.e., the intensity fluctuations) is recorded with a sampling frequency of 10^3 to 10^4 . Along the propagation path, turbulent eddies of different sizes and thermodynamic characteristics cause scattering of the electromagnetic signal, which is, therefore, highly variable in time. also shows several length scales that are important in connection with the analysis and interpretation of scintillometer measurements. These

are: The length of the scintillometer path (X) The (effective) height of the path above ground. The outer and inner scale lengths of turbulence L_0 and l_0 , respectively, where L_0 marks the transition between the production and inertial ranges of the turbulence spectrum that usually scales with z , and l_0 marks the transition between the inertial and dissipation ranges of the turbulence spectrum, it typically amounts to a few mm. The aperture of the transmitter and receiver units (in principle, they might be different, but for most systems, $D(\text{transmitter}) = D(\text{receiver})$).

2.3. TYPES OF SCINTILLOMETER

There are 4 types of scintillometers

1. Optical Small Aperture Scintillometer
2. Optical Large Aperture Scintillometer
3. Laser Scintillometer
4. Microwave Scintillometer

2.3.1. OPTICAL SMALL APERTURE SCINTILLOMETER

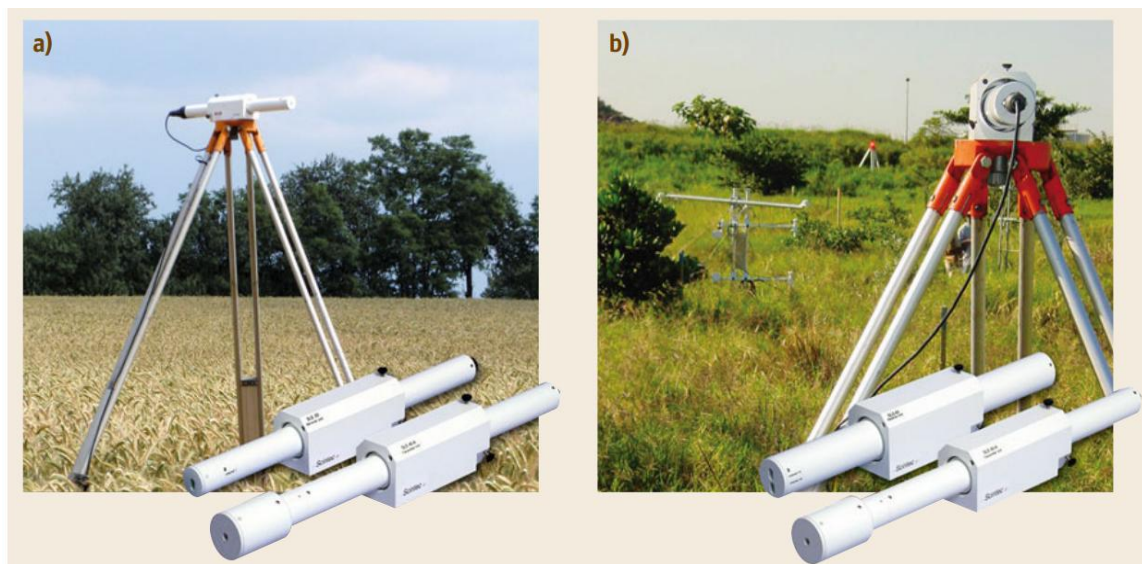


FIGURE 2.2. (a & b) Optical Small Aperture Scintillometers

Optical dual-beam, small-aperture laser scintillometers (DBLS), are called surface-layer scintillometers (SLS). Basic application is the determination of the turbulent fluxes of sensible heat and momentum at the field scale. They are generally operated within the atmospheric surface layer. SLS systems operate with visible laser light at 670 nm wavelength (red light); The SLS20 (Fig. 2.2) is the basic version, and the SLS40 has implemented special features to correct for possible vibrations of the mounting platforms (e.g., towers), while the A-version of both types offers automatic beam steering, a feature especially suited for operation on soft ground. Special features implemented with the system hardware and software include Radiation modulation for background elimination and interference filter for use in direct

sunlight. Real-time data monitoring includes raw data and fluxes and amplitude and statistical tests on the mean and scintillation signals resulting in an internal data quality assessment.

2.3.2. OPTICAL LARGE APERTURE SCINTILLOMETER

In 2001, LAS MkI instrument was developed, in which the signal is created by one single LED, and a Fresnel lens is used both at the transmitter and receiver sides to form the beam and to focus the received signal on a photodiode. This instrument was redesigned in 2012, resulting in the LAS MkII. The LAS MkII Scintillometer provides continuous measurements of sensible heat fluxes over path lengths from 100 m up to 4.5 km.

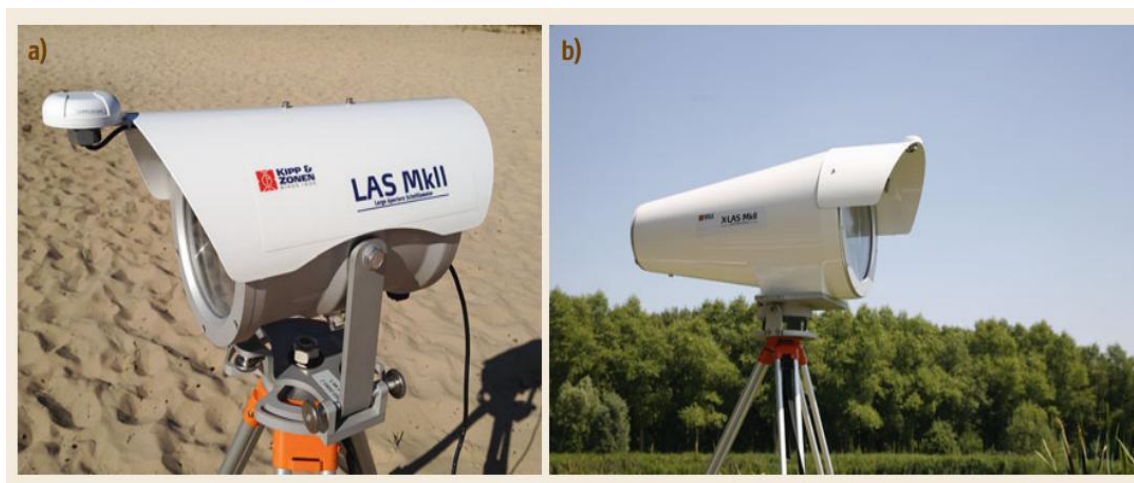


FIGURE 2.3 (a & b) Optical Large Aperture Scintillometer

The C_n^2 data and demodulated signal are also available. The standard operating range of the LAS is 0.25-4.5 km, but this can be reduced to 0.1-1 km using the included reduction aperture. The transmitter signal originates from a large number of LEDs arranged on one (BLS450) or two disk(s) (BLS900, BLS2000), the transmitter divergence resulting in a quite large illuminated area with increasing path length. This reduces the sensitivity to misalignment or instability of the mounting structures.

At the receiver side, a glass or Fresnel lens acts to focus the signals on two photodiodes. It is an extra-large aperture scintillometer (XLAS). In 2018, a new version of the extra-large aperture scintillometer (XLAS) MkII was released extending the range to 12 km.

2.3.3 LASER SCINTILLOMETER

Froehlich (1992) used divergent lasers (DLS) and Thiermann (1992) designed a displaced-beam laser scintillometer (DBLS) both providing the inner scale l_0 , which

is directly related to the dissipation rate of turbulent kinetic energy \mathcal{E} , as well as the structure parameter of refractive index C_n^2 . The spectrum of refractive index variations in the so-called dissipation range obeys the theory developed by Hill (1998).



FIGURE 2.4. Laser Scintillometer

The single divergent laser beam scintillometer has been used by Frehlich with different detectors placed perpendicular to the central axes of the diverged light beam. This concerns the case of a point source. The transmitter of a displaced-beam laser scintillometer (DBLS) is a red-light laser with a beam-splitter creating 2 orthogonal polarized beams. For distances between 50 m and 250 m DBLS laser scintillometers are used.

For larger distances up to 12 km Boundary Layer Scintillometers (BLS) are used. The turbulence close to the ground is measured at a height of 1.2 m above the ground at a horizontal distance of 75 m at a wavelength of 670 nm. Heat flux and momentum flux are estimated by purely optical means.

2.3.4 MICROWAVE SCINTILLOMETER

Scintillometers operating at wavelength $\lambda \sim 1-19$ mm are called microwave scintillometers (MWS). In 2014 commercially available microwave Scintillometer **RPG-MWSC-160** was designed for combined operation with an optical Large Aperture Scintillometer (LAS) to observe sensible and latent heat fluxes at the same time. The MWSC-160 transmitter projects a beam of 160.8 GHz radiation over a path length from 500 to 10 km to a receiver with an aperture of 300 mm.



FIGURE 2.5: Microwave Scintillometer

2.4 PARAMETERS MEASURED

1. **C_m , the structure constant of refractive index fluctuations**: The magnitude of the refractive index, which is the spectral amplitude of refractive index fluctuations in the inertial subrange of turbulence.
2. **Sensible heat flux**: Measurements of the transfer of heat between the Earth's surface and the air above, called the sensible heat flux.
3. **Momentum flux**: Measures the dissipation rate of turbulent kinetic energy, the momentum flux, as these can measure the inner scale of refractive index fluctuations of the smallest size of eddies.

Scintillometer type	Measured variable	Derived atmospheric variable	Symbol and unit
Single-beam optical scintillometer	Variance of electromagnetic signal intensity	Structure parameter of temperature Sensible heat flux density	C_{TT} in $K^2 m^{-2/3}$ Q_H in $W m^{-2}$
Combined optical-microwave scintillometer	Variances and covariance of optical/microwave signal intensities	Structure parameters of temperature and humidity Sensible and latent heat flux densities	C_{TT} in $K^2 m^{-2/3}$ C_{qq} in $kg^2 m^{-6} m^{-2/3}$ C_{Tq} in $K kg m^{-3} m^{-2/3}$ Q_H in $W m^{-2}$ Q_E in $W m^{-2}$

TABLE 2.1: Types of Scintillometer - Measured variables

2.4.1 INTENSITY FLUCTUATIONS - THE VARIANCE

- Intensity fluctuations are mathematically expressed as the Variance.
- The refractive index structure parameter, C_{nn} , can be related to parameters of temperature and humidity, C_{TT} , C_{qq} , and C_{Tq} .
- The relative contribution of temperature and humidity fluctuations to the refractive index, depends on the wavelength of the radiation.
- Temperature fluctuations dominate in the visible and near-infrared spectral range (wavelengths typically between 400 nm and 4 μ m). Humidity fluctuations become relevant for millimeter waves (wavelength 1-20 mm)

2.5. SCINTILLOMETRY EQUATIONS

$$\sigma_{ln(A)}^2 = \frac{1}{4} \ln \left(\frac{\sigma_I^2}{I^2} + 1 \right) \quad \text{----->Eq 2.1}$$

$$C_{nn}(\text{LAS}) = 4.48 \sigma_{ln(A)}^2 D^{\frac{7}{3}} X^{-3} \quad \text{----->Eq 2.2}$$

$$c_{nn}(\text{MWS}) = 8.06 \sigma_{ln(A)}^2 k^{\frac{-7}{6}} x^{\frac{-11}{6}} \quad \text{----->Eq 2.3}$$

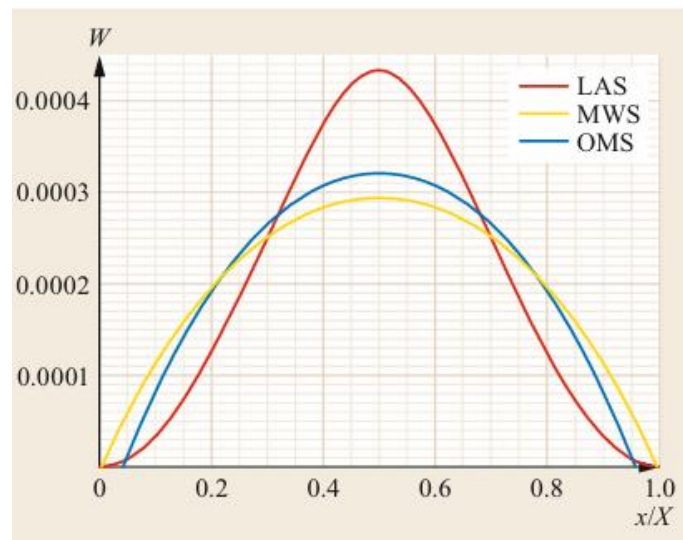


FIGURE 2.6: Scintillation spectra from simultaneous LAS and MWS measurements

Scintillometry is used in real-time in combination with remote sensing techniques to estimate large-scale evaporation and soil moisture using skin temperature derived from satellites. Considering the skill of the LAS it is worthwhile to promote the use of LAS as an operational instrument in meteorological and hydro-meteorological networks. Laser scintillometers in combination with additional net radiation and soil heat flux might be suitable for agricultural fields.

CHAPTER - 3

LASER SCINTILLOMETER EXPERIMENTATION

3.1 INTRODUCTION

The concept of LASER beam was first presented by “**Albert Einstein**” in **1917**. The word laser is an acronym that stands for “**Light Amplification by the Stimulated Emission of Radiation**”. It is a device for producing a very narrow beam of highly intensive monochromatic coherent light. LASER Light is an electromagnetic wave with the following properties.

3.1.1 LASER PROPERTIES

The characteristics of laser beam are

1. Monochromaticity
2. Coherency
3. Low divergence

3.1.2 PRINCIPLE OF LASER

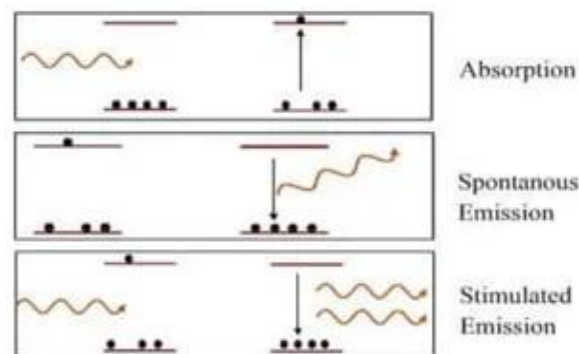


FIGURE 3.1: Principle of Laser

1. The process of exciting the atom to a higher energy level by absorbing the stimulating incident photons known as stimulated absorption of radiation.
2. The transition of an excited atom by itself to a lower energy level is known as spontaneous emission of radiation.
3. The excited atom after getting stimulated by the incident photon transits to a lower energy level by emitting photons is known as the stimulated emission of radiation.

3.2 CLASSIFICATION OF LASER BY METHOD OF GENERATION

Gas Lasers: Examples include helium-neon (HeNe) lasers, carbon dioxide (CO₂) lasers, and Argon ion lasers. Gas lasers use gas as the active medium and are often

used in scientific research, medical procedures, and industrial applications like cutting and welding.

Solid-State Lasers: These lasers use solid materials as the gain medium, such as crystals (ruby, neodymium-doped yttrium aluminum garnet - Nd:YAG), glasses, or semiconductors. Solid-state lasers are versatile and find applications in medicine (laser surgery), telecommunications (fiber lasers), and manufacturing.

Semiconductor Lasers: Known as diode lasers, they use semiconductor materials like gallium arsenide as the gain medium. Semiconductor lasers are widely used in consumer electronics (DVD players, laser pointers), telecommunications (fiber optics), and medical devices.

Fiber Lasers: These lasers use optical fibers as the gain medium and can achieve high power and efficiency. Fiber lasers are commonly used in industrial cutting and welding, telecommunications, and military applications.

Dye Lasers: Dye lasers use organic dye molecules dissolved in a solvent as the gain medium. They offer tunable wavelengths and are used in scientific research, spectroscopy, and medical treatments.

3.3. APPLICATIONS OF LASERS

Medicine: Laser surgery (ophthalmology, dermatology, dentistry), cosmetic procedures (hair removal, tattoo removal), diagnostics (imaging techniques like MRI and PET scans).

Manufacturing: Laser cutting, welding, drilling, marking, engraving in industries such as automotive, aerospace, electronics.

Communications: Optical fibers and semiconductor lasers enable high-speed data transmission in telecommunications networks, internet infrastructure, and fiber-optic sensors.

Entertainment: Laser light shows, laser projectors in theaters, clubs, and events.
Research: Laser spectroscopy, microscopy, atomic and molecular physics experiments, laser cooling and trapping of atoms for quantum studies.

3.4 SELECTION OF MODULES FOR INSTRUMENTATION

3.4.1 LASER SOURCE

NARL Lidar Lab possesses two low energy CW laser sources for the alignment of their high energy LIDAR's optical instruments. One low energy laser is operating at 532 nm and the other is at 633 nm. The 633 nm laser has the special features of stable output energy/wavelength option. Hence, this laser is selected to perform Scintillometer experimentation with stable output energy

This helium-neon (He-Ne) laser is a gas laser that uses a mixture of helium and neon gas as its gain medium. The mixture is contained in a sealed glass tube at a low pressure, with a ratio of helium to neon ranging from 5:1 to 20:1. The laser is excited by an electrical discharge through an anode and cathode at each end of the tube. The optical cavity consists of a flat mirror at one end and a concave output coupler mirror at the other.

The most well-known He-Ne laser operates at a wavelength of 632.8 nm, in the red part of the visible spectrum. The laser's excitation mechanism involves electrons colliding with helium atoms to produce helium metastable atoms, which then transfer their energy to neon laser levels.



FIGURE 3.2: He-Ne Laser

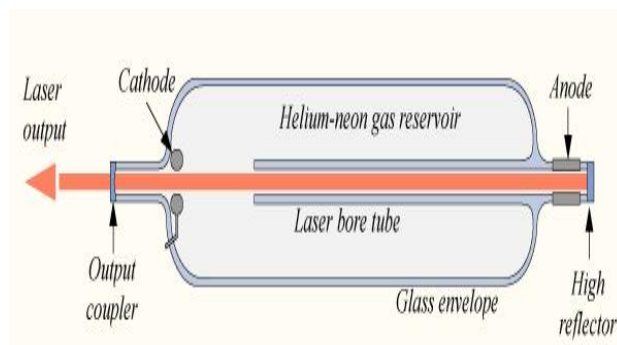


FIGURE 3.3: Internal structure of He-Ne Laser

3.4.1.1 SPECIFICATIONS OF HE-NE LASER

1. Center Wavelength: 632.992 nm
2. Offers Two Stabilization Modes: Frequency or Intensity
3. Output Power > 1.2 mW
4. Beam Diameter: 0.65 ± 0.05 mm
5. Linearly Polarized Output

6. Time to Lock :<15 Minutes
7. Temperature Range to Maintain Lock: 15–30°C

3.4.1.2 ADVANTAGES OF LOW POWER LASER

1. **Eye Safety:** Low-power lasers are typically classified as Class 1 lasers, which are considered safe for human exposure under normal operating conditions. This ensures that scintillometer measurements can be conducted without posing a risk to personnel.
2. **Regulatory Compliance:** Many countries have regulations regarding laser safety, especially in public or populated areas. By using a low-power laser, scintillometer operators can comply with these regulations more easily, reducing regulatory hurdles for deployment.
3. **Cost-effectiveness:** Low-power lasers are generally less expensive to operate and maintain compared to high-power lasers. They consume less energy and have longer lifespans, resulting in lower operational costs for scintillometer systems.
4. **Reduced Environmental Impact:** Lower power lasers have a reduced environmental impact, both in terms of energy consumption and potential hazards. This aligns with sustainability goals and minimizes the ecological footprint of scintillometer operations.
5. **Improved Portability:** Low-power laser-based scintillometers can be designed to be more compact and lightweight, enhancing their portability and ease of deployment in field settings. This is advantageous for mobile monitoring applications or studies in remote areas.
6. **Less Interference:** Low-power lasers are less likely to interfere with other sensitive equipment or communication systems, reducing the risk of electromagnetic interference (EMI) and ensuring accurate data acquisition without external disturbances.
7. **Longer Operating Lifespan:** The components of low-power laser systems often have longer operating life spans due to reduced stress and wear. This translates to more reliable and durable scintillometer systems with fewer maintenance requirements over time.

3. 4. 2 PHOTO DETECTOR

Photodetectors, also called photosensors, are sensors of light or other electromagnetic radiation. There are a wide variety of photodetectors which may be classified by mechanism of detection, such as photoelectric or photochemical effects, or by various performance metrics, such as spectral response. Semiconductor-based photodetectors typically use a p–n junction that converts photons into charge. The absorbed photons make electron–hole pairs in the depletion region. Photodiodes and phototransistors are a few examples of photo detectors. Solar cells convert some of the light energy absorbed into electrical energy. The photomultiplier tubes are other types of sensitive receiving systems for Laser beam analysis.

Another laser energy meter in the low energy lab, ‘Star-Lite low power energy meter’ is explored to detect the received laser beam. This system needed calibrations and hence could not be used.



FIGURE 3.4: Photo Detector

3.4.2.1 SPECIFICATIONS OF PHOTO DETECTOR

1. Spectral Range: 200-1100 nm
2. Active Area: Typically 2-5mm²
3. Responsivity: Around 0.4 A/W at 800 nm.
4. Dark Current: Typically, less than 100 pA at a bias voltage of 5V.
5. Bias Voltage: Typically operated at 5V.
6. Capacitance: Around 10 pF.
7. Rise Time/Fall Time: Approximately 20 ns.

3.4.3 OSCILLOSCOPE

The option of high energy meters to detect Scintillometer CW low power laser beams is explored. But the sensitivity of the available high energy laser measuring energy meters is so coarse, that the energy meter did not sense the low power energy of the scintillometer experiment. Hence, the photodetector of the high energy laser energy meter along with the light diffuser to safeguard the sensitive detector connected to the Oscilloscope is finalized for the Scintillometer experimentation.

A latest digital oscilloscope is a electronic test instrument that graphically displays varying voltages of one or more signals as a function of time. Their main purpose is capturing information on electrical signals for debugging, analysis, or characterization. The displayed waveform can then be analyzed for properties such as amplitude, frequency, rise time, time interval, distortion, and others. Originally, calculation of these values required manually measuring the waveform against the scales built into the screen of the instrument. Modern digital instruments may calculate and display these properties directly.



FIGURE 3.5: OSCILLOSCOPE

Oscilloscopes are used in the sciences, engineering, biomedical, automotive and the telecommunications industry. General-purpose instruments are used for maintenance of electronic equipment and laboratory work. Special-purpose oscilloscopes may be used to analyze an automotive ignition system or to display the waveform of the heartbeat as an electrocardiogram, for instance.

The oscilloscope has a special feature to sample the input data and store it in digital format on the USB. this feature is used. The standard data size is 1000-point series. The time base is adjusted to collect 1000 point dataset in 90 sec. period, so that the data file is created every 90 sec manually. The data recording files are created manually for a two hour period for each experiment. Each dataset consists of approximately 25 files per hour.

3.4.3.1 SPECIFICATIONS OF OSCILLOSCOPE

1. Bandwidth: 500 MHz.
2. Input Impedance: $1\text{ M}\Omega \pm 1\%$.
3. Maximum Input Voltage: 300 V rms .
4. Trigger Modes: Edge, Pulse Width, Video, Pattern, Delay, Time-out, USB.
5. Connectivity: USB, LAN, GPIB (optional).
6. Rise Time: $\leq 700\text{ ps}$.
7. Time Base Range: 2 ns/div to 50 s/div.
8. Operating Temperature: 0°C to $+50^{\circ}$.

CHAPTER - 4

METHODOLOGY FOR MEASURING PARAMETERS

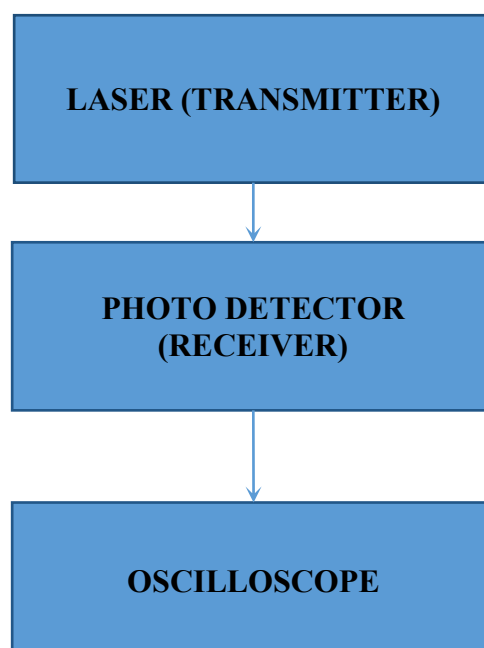
4.1 PROCESS

In our project, we embark on a comprehensive exploration of atmospheric dynamics, focusing on the recording of temperature and heat flux within various environmental contexts. Our methodology involves a meticulously crafted experimental setup, leveraging sophisticated instrumentation and data acquisition techniques to unravel the mysteries of the atmosphere.

At the heart of our endeavor lies the utilization of cutting-edge technology, namely a laser as our primary transmitter and a photodetector as the receiver. This pairing forms the cornerstone of our data collection strategy, allowing us to probe the atmospheric medium with precision and accuracy. The photodetector is positioned in the path of the laser beam, with carefully calibrated distances ranging from a mere 1 meter to a substantial 60 meters separating the two components.

The process begins with the activation of our experimental apparatus, initiating a continuous stream of data collection spanning a duration of 1 to 2 hours. Each iteration of data collection yields a wealth of information, with no less than 1000 data points meticulously captured and archived at regular intervals of 90 seconds. This relentless pursuit of data acquisition ensures a robust dataset, teeming with insights waiting to be unearthed.

4.2. BLOCK DIAGRAM



4.3. LASER INTENSITY MEASUREMENT EXPERIMENTS:

Experiment	LASER-DETECTOR Beam path distance, height	Mean amplitude (V)	Mean of Std. deviation values of total expt.
On optical bench, Small distance	1 m, 20 cm	0.253	0.0018973
Lab Room to Room	3.4 m, 1.1 m	0.1880363	0.0018341
Room to Room by creating turbulence	3.4 m, 1.1 m	0.186153	0.002169
Outdoor environment	20 m, 2 m	0.091894	0.002292
Outdoor building to building	60 m, 5 m	0.104819	0.001907

TABLE 4.1: Overview of Calculations

Our experimental scenarios encompass a diverse array of environments, ranging from controlled laboratory settings to real-world outdoor conditions. Within the confines of a single room, we meticulously change the distances between the transmitter and receiver, scrutinizing the impact of spatial separation on signal characteristics. Furthermore, we extend our investigation to encompass inter-room dynamics, examining the influence of turbulence on signal propagation.

Beyond the confines of the laboratory, our explorations traverse a vast landscape of environmental diversity, encompassing everything from humble huts to towering buildings. Each locale presents its own unique set of challenges and opportunities, offering a rich tapestry of atmospheric phenomena waiting to be deciphered.

Central to our analytical approach is the computation of key statistical metrics, namely the mean and standard deviation of the collected data. These fundamental measures serve as the bedrock upon which our subsequent analyses are built, providing invaluable insights into the underlying trends and variations within our dataset.

Armed with a treasure trove of data and a robust analytical framework, we embark on the arduous task of deriving meaningful insights from our observations.

Through the judicious application of mathematical models and statistical techniques, we endeavor to unlock the secrets of the atmosphere, unraveling the complex web of interactions that govern its behavior.

At the heart of our analysis lies the quest to derive crucial atmospheric parameters such as temperature and heat flux. These fundamental metrics serve as the linchpin of our understanding, offering a glimpse into the inner workings of the atmosphere and its myriad complexities.

4.3.1. LASER BEAM PROPAGATION WITHIN LASER LAB - BETWEEN TWO ROOMS



FIGURE 4.1 : Experimental Setup



FIGURE 4.2 : Photo Detector



FIGURE 4.3: Oscilloscope

The above figures 4.1, 4.2, 4.3 show setting up an experiment across two rooms separated by 3.14 meters at a height of 1.1 meters. One room housed the laser source, while the other contained the photo detector connected to an oscilloscope for voltage measurement. Data collection performed over 3 hours, with readings taken every 90 seconds. The experiment was divided into two phases: the initial 1.5 hours at room

temperature and the remaining time with induced turbulence using an air conditioner. This setup aimed to analyze how turbulence affects refractive index, crucial for atmospheric and environmental studies.

The objective was to understand turbulence's impact on radiations, particularly over short distances. By measuring voltage changes during turbulence compared to stable conditions, insights were gained into radiation behavior in varying environments. This experiment's findings are significant for applications in atmospheric science, environmental monitoring, and remote sensing, highlighting the importance of considering turbulence effects in radiation studies for accurate data interpretation and modeling.

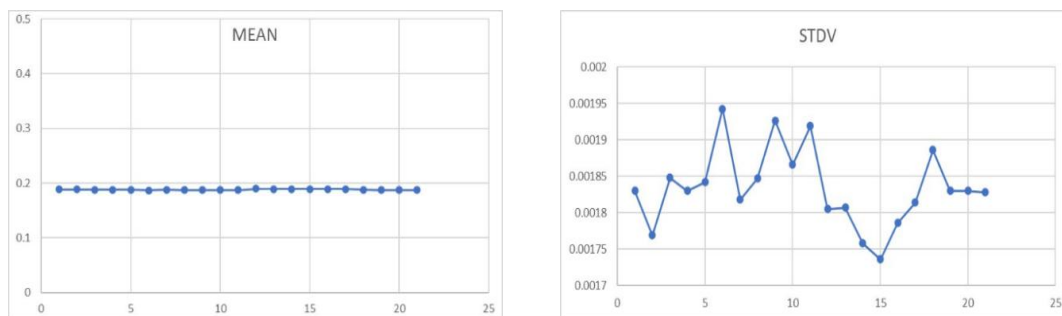


FIGURE 4.4: Mean and Standard Deviation Graphs for Room to Room Readings at Room Temperature

After meticulously collecting voltage data at 90-second intervals, we performed statistical analysis by calculating mean and standard deviation for each interval, unveiling insights into central tendency and variability of the radiation signal over time. This process allowed us to discern trends and fluctuations within the data. By computing the average mean and standard deviation across all intervals, we obtained a comprehensive overview of the evolution of voltage readings throughout the experiment, capturing the overall behavior of the radiation signal under the specific conditions tested.

To aid in interpretation, we graphed mean voltage values over time (x-axis: time, y-axis: average voltage mean) shown by figure 4.4 and standard deviations of mean voltage readings (x-axis: time, y-axis: average standard deviation) shown by figure 4.4, providing visual representation of the signal's dynamics, fluctuations, and response to environmental conditions, enhancing our understanding of its variability and behavior.

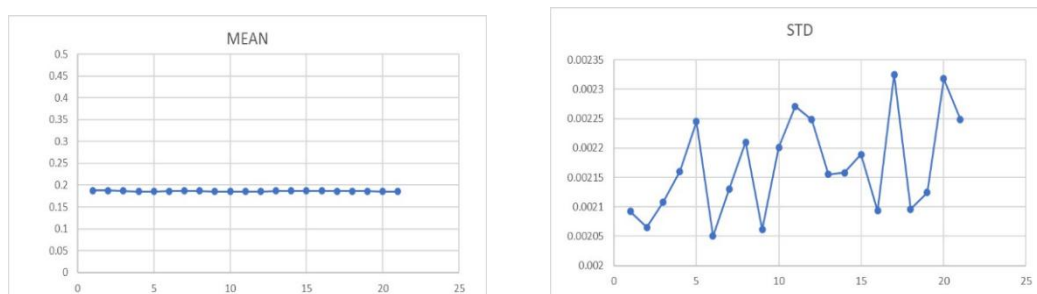


FIGURE 4.5: Mean and Standard Deviation Graphs for Room-to-Room Readings With the Creation of Turbulence by Switching on the Air Conditioners

Continuing the experiment at a varying room temperature to 20 degrees Celsius and 30 degrees Celsius repeatedly, by frequently switching on and off the air conditioner, by switching on the AC louvers fins in the oscillation mode, we applied continuous turbulence in the laser beam path to collect the voltage data. By calculating the mean and standard deviation for each 90-second interval of voltage readings under the new temperature setting, we gained insights into the central tendencies and variability specific to the turbulent air movement condition in the Lab. To visually compare the results, we plotted two additional graphs (4.5) one depicting the mean voltage values over time and another illustrating the standard deviations of the mean voltage readings. These graphs facilitated a comparative analysis between the radiation signal's behavior contributing to a deeper understanding of how temperature variations affect radiation propagation and signal stability. The standard deviation values have increased considerably in the measured results with turbulence.

4.3.2 LASER BEAM PROPAGATION IN OUTDOOR ENVIRONMENT



FIGURE 4.6: Experimental Setup from Hut to Hut

In the outdoor environment, we attempted to propagate a laser beam from the flux tower region to a 50-m tower, which is spanning about 100m. Due to the bright sunlight and considerable distance, we could not place the photodetector rx instrumentation in the laser beam path. Hence, as shown in figure (4.6), we devised the experimental setup spanning from hut to hut, limiting the distance of the laser beam to 20 m, at a height of 2 meters on masts. The setup involved placing a laser source near one hut, exposed to direct sunlight, and a photodetector near the other hut, in sunlight. Through the connection of an oscilloscope to the photo detector, we meticulously recorded voltage data at 90-second intervals over a duration of 1 hour. Conducting the experiment outdoors in sunlight ensured natural turbulence, a crucial factor in our observations. This setup allowed us to study the scintillation phenomenon, with variations in radiation intensity caused by atmospheric turbulence.

Following the setup and data collection process, we analyzed the voltage data by computing the mean and standard deviations for each 90-second interval. Utilizing this processed data, we generated two distinct graphs shown in figure 4.7, similar to the previous graphs showing mean and standard deviation of laser beam intensity. These graphs provide a visual representation of the fluctuations in mean voltage and its associated variability throughout the duration of the experiment, offering insights into the dynamics of the natural turbulence phenomena.

This outdoor environment experiment is considered unsafe to the sensitive lab based photodetector due to bright ambient light, and the ambient temperature of 40 degrees which is considered unsafe for the laser source. The light diffuser safeguarded the photodetector and the heat dissipation of source to the mast protected the laser source. Hence, it is planned to keep the sensitive instruments in the environment controlled labs, by propagating laser beams in the open space in consequent experiments.

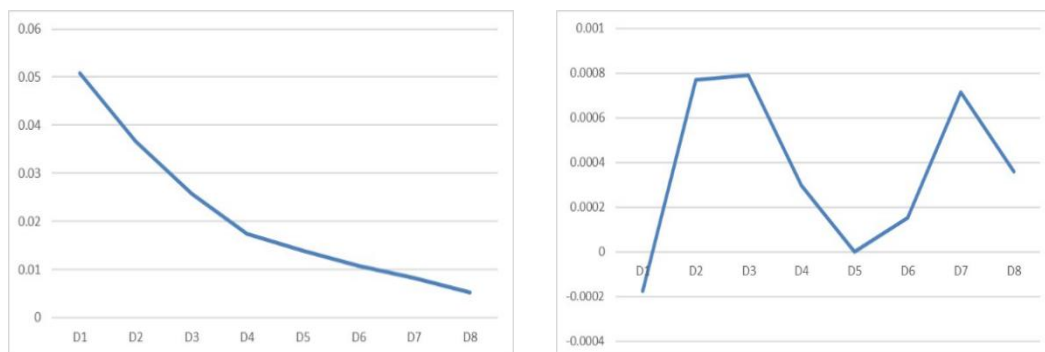


FIGURE 4.7: Mean and Standard Deviation Graphs for Outdoor Environment

4.3.3 LASER BEAM PROPAGATION BETWEEN BUILDINGS

To form the outdoor setup, we devised an experiment spanning from one building to another, covering a distance of approximately 60 meters with a height of 5 meters. The setup involved positioning a laser source in one building and a photo detector in another, both in an air conditioned environment. The laser beam is passed over the ambient environment over the lawn, rock and road etc. Figure 4.8. a. shows the laser beam position and 4.8. b shows the laser source and beam spot from outside the building. Figure 4.9 presents the landscape of the beam path consisting of the lawn, rock and road etc. The photodetector lab laser beam imprint on the wall in darkness is shown in figure 4.10. It is observed that the beam diameter increased, even with the lowest specification of the divergence of the laser source, as the distance is considerable. The photodetector is placed in the beam path and digital data is collected, as shown in the figure 4.11. Through the connection of an oscilloscope to the photo detector, we meticulously gathered voltage data at 90-second intervals over a duration of 3 hours. Each interval comprised approximately 1000 samples of voltage. This comprehensive data collection allowed us to thoroughly examine the fluctuations in voltage over time, providing dynamics of natural atmospheric turbulence and its impact on laser beam intensity.

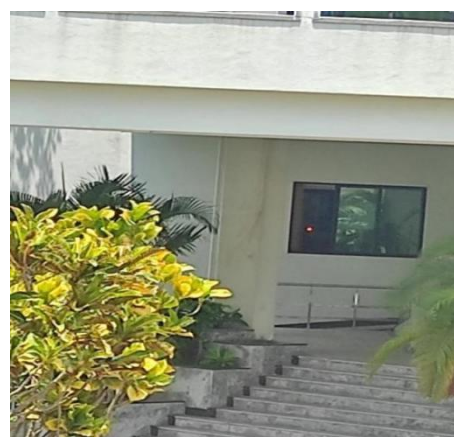
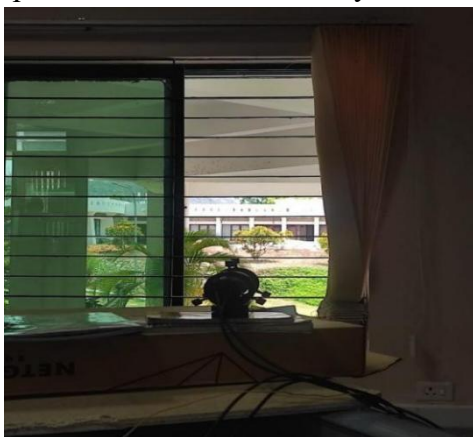


FIGURE 4.8 a, b: Laser source in the building



FIGURE 4.9: Landscape



FIGURE 4.10: Laser beam spot



FIGURE 4.11: Photo Detector in the Building

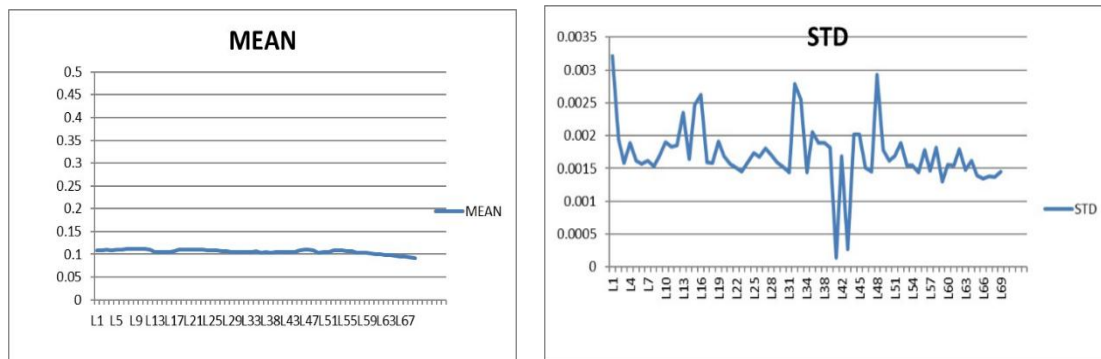


Fig 4.12: Mean and Standard Deviation graphs for Building to Building readings

Figure 4.12 presents the mean and standard deviation data plots of the final experiment. Utilizing this processed data, we generated two distinct graphs. The first graph illustrates the mean voltage over time, with the x-axis denoting the 90-second intervals and the y-axis representing the mean voltage.

These data sets are used to find the refractive index structure constant C_n^2 .

CHAPTER - 5

RESULTS

5.1 ROOM TO ROOM VALUES AT ROOM TEMPERATURE

In our experiments, the laser beam intensity values are measured at every 100 millisecond time period. Each file consists of 1000 point data series. 1000-point time series data of 90 sec time is stored in each data file. The file name/number creation is performed manually in the oscilloscope/USB storage after collection of 90 sec data. Hence, about 25-30 data files are created manually within one hour.

Subsequently, we calculated the atmospheric refractive index structure parameter (C_n^2) for each interval of 90 sec data, using the LAS (Large aperture scintillometer) formula available in the literature that is presented in equations 2.1 and 2.2. The variance, beam path distance and beam aperture are taken as per the experimental setups used in table 4.1.

Table 5.1 presents the C_n^2 values obtained with the experiment conducted in the lab environment.

FILE NAME	MEAN	STDV	σ^2	I^2	$\sigma^2 \ln(A)$	C_n^2
1	0.18855	0.00183	3.3489E-06	0.035551	2.35488E-05	2.00224E-05
2	0.18821	0.001769	3.1294E-06	0.035423	2.20847E-05	1.87775E-05
3	0.18794	0.001848	3.4151E-06	0.035321	2.41704E-05	2.0551E-05
4	0.18778	0.00183	3.3489E-06	0.035261	2.37423E-05	2.01869E-05
5	0.18763	0.001842	3.393E-06	0.035205	2.40932E-05	2.04852E-05
6	0.18673	0.001942	3.7714E-06	0.034868	2.70388E-05	2.29897E-05
7	0.18766	0.001818	3.3051E-06	0.035216	2.34619E-05	1.99486E-05
8	0.18749	0.001847	3.4114E-06	0.035153	2.42603E-05	2.06274E-05
9	0.18749	0.001926	3.7095E-06	0.035153	2.63799E-05	2.24296E-05
10	0.18735	0.001866	3.482E-06	0.0351	2.4799E-05	2.10854E-05
11	0.18749	0.001919	3.6826E-06	0.035153	2.61885E-05	2.22668E-05
12	0.18951	0.001805	3.258E-06	0.035914	2.26783E-05	1.92823E-05
13	0.18913	0.001807	3.2652E-06	0.03577	2.282E-05	1.94027E-05
14	0.18922	0.001758	3.0906E-06	0.035804	2.15787E-05	1.83473E-05
15	0.189173	0.001736	3.0137E-06	0.035786	2.10525E-05	1.78999E-05
16	0.18897	0.001786	3.1898E-06	0.03571	2.23305E-05	1.89865E-05
17	0.18892	0.001814	3.2906E-06	0.035691	2.30483E-05	1.95968E-05
18	0.18812	0.001886	3.557E-06	0.035389	2.51265E-05	2.13638E-05
19	0.18728	0.00183	3.3489E-06	0.035074	2.38692E-05	2.02949E-05
20	0.18717	0.00183	3.3489E-06	0.035033	2.38973E-05	2.03187E-05
21	0.18695	0.001828	3.3416E-06	0.03495	2.39013E-05	2.03221E-05

H	D	X	$D^{7/3}$	X^{-3}	Avg
1.1m	0.00033	0.00341	7.52545E-09	25219522.7	2.02469E-05

TABLE 5.1: Room to Room (at room temperature)
This data set presents the C_n^2 average value of 2.02469e-05.

5.2 ROOM TO ROOM VALUES BY CREATING TURBULENCE

Table 5.2 presents the C_n^2 values obtained with the experiment conducted in the lab environment with turbulence creation. This data set presents the C_n^2 average value of $4.00554\text{e-}06$.

FILE NAME	MEAN	STD	σ^2	I^2	$\sigma^2 \ln(A)$	C_n^2
1	0.18786	0.002092	4.37646E-06	0.03529138	3.10004E-05	3.7211E-06
2	0.1877	0.002065	4.26423E-06	0.03523129	3.0257E-05	3.6257E-06
3	0.18666	0.002108	4.44366E-06	0.034841956	3.18824E-05	3.7782E-06
4	0.18562	0.00216	4.6656E-06	0.034454784	3.38508E-05	3.9669E-06
5	0.18502	0.002245	5.04003E-06	0.0342324	3.68047E-05	4.2853E-06
6	0.18614	0.00205	4.2025E-06	0.0346481	3.03209E-05	3.5732E-06
7	0.18689	0.00213	4.5369E-06	0.034927872	3.24712E-05	3.8575E-06
8	0.18656	0.00221	4.8841E-06	0.034804634	3.50798E-05	4.1527E-06
9	0.18555	0.002061	4.24772E-06	0.034428803	3.08423E-05	3.6116E-06
10	0.1851	0.002201	4.8444E-06	0.03426201	3.53457E-05	4.119E-06
11	0.1853	0.002271	5.15744E-06	0.03433609	3.75483E-05	4.3851E-06
12	0.18562	0.002248	5.0535E-06	0.034454784	3.6665E-05	4.2967E-06
13	0.18674	0.002155	4.64403E-06	0.034871828	3.32913E-05	3.9486E-06
14	0.18673	0.002158	4.65696E-06	0.034868093	3.33876E-05	3.9596E-06
15	0.18655	0.002189	4.79172E-06	0.034800903	3.442E-05	4.0742E-06
16	0.18654	0.002093	4.38065E-06	0.034797172	3.14708E-05	3.7247E-06
17	0.18645	0.002325	5.40563E-06	0.034763603	3.88711E-05	4.5961E-06
18	0.18604	0.002096	4.39322E-06	0.034610882	3.17309E-05	3.7353E-06
19	0.18575	0.002124	4.51138E-06	0.034503063	3.26861E-05	3.8358E-06
20	0.1852	0.002318	5.37312E-06	0.03429904	3.91607E-05	4.5685E-06
21	0.1852	0.002249	5.058E-06	0.03429904	3.68642E-05	4.3006E-06

H	D	X	$D^{7/3}$	X^{-3}	Avg
1.1m	0.00033	0.00341	7.52545E-09	25219522.7	4.00554E-06

TABLE 5.2: Room to Room (with some Turbulene)

5.3 OUTDOOR ENVIRONMENT

Table 5.3 presents the C_n^2 values obtained with the experiment conducted in the outdoor environment with natural turbulence. This data set presents the C_n^2 average value of $7.46\text{e-}06$.

FILE NAME	MEAN	STDV	σ^2	I2	$\sigma^2 \ln(A)$	Cnn
D1	0.05033	-0.000173	3.01023E-08	0.002533109	2.97086E-06	5.05154E-08
D2	0.03667	0.0007705	5.9367E-07	0.001344689	0.000110349	1.87633E-06
D3	0.02579	0.0007925	6.28056E-07	0.000665124	0.000235956	4.0121E-06
D4	0.01744	0.0002985	8.91023E-08	0.000304154	7.32271E-05	1.24513E-06
D5	0.01399	0.0000275	7.5625E-10	0.00019572	9.65982E-07	1.64252E-08
D6	0.01076	0.0001545	2.38703E-08	0.000115778	5.1538E-05	8.76332E-07
D7	0.00821	0.0007135	5.09082E-07	6.74041E-05	0.001881078	3.19851E-05
D8	0.00532	0.0003615	1.30682E-07	2.83024E-05	0.001151682	1.95827E-05

H	D	X	D^{7/3}	X⁻³	Avg
2m	0.0006	0.02	3.03636E-08	125000	7.46E-06

TABLE 5.3: Hut to Hut

5.4 BUILDING TO BUILDING

Table 5.4 presents the C_n^2 values obtained with the experiment conducted in the lab environment with natural turbulence with the long distance laser propagation. This data set presents the C_n^2 average value of 8.72484e-07.

FILE NAME	MEAN	STD	σ^2	I²	$\sigma^2 \ln(A)$	C_n^2
L1	0.1082	0.003212	1.03169E-05	0.01170724	0.000220214	1.17638E-06
L2	0.10919	0.001951	3.8064E-06	0.011922456	7.98031E-05	4.26308E-07
L3	0.10945	0.001587	2.51857E-06	0.011979303	5.25553E-05	2.80751E-07
L4	0.1078	0.001889	3.56832E-06	0.01162084	7.67538E-05	4.10019E-07
L5	0.1093	0.001613	2.60177E-06	0.01194649	5.44404E-05	2.9082E-07
L6	0.10987	0.001573	2.47433E-06	0.012071417	5.12383E-05	2.73715E-07
L7	0.11215	0.001622	2.63088E-06	0.012577623	5.22875E-05	2.7932E-07
L8	0.11219	0.001531	2.34396E-06	0.012586596	4.65524E-05	2.48683E-07
L9	0.112	0.001686	2.8426E-06	0.012544	5.66461E-05	3.02603E-07
L10	0.11128	0.001901	3.6138E-06	0.012383238	7.29469E-05	3.89682E-07
L11	0.11093	0.001829	3.34524E-06	0.012305465	6.79533E-05	3.63006E-07
L12	0.10924	0.001855	3.44103E-06	0.011933378	7.20779E-05	3.8504E-07
L13	0.10584	0.002355	5.54603E-06	0.011202106	0.000123741	6.61026E-07
L14	0.10539	0.001646	2.70932E-06	0.011107052	6.09745E-05	3.25726E-07
L15	0.10555	0.002471	6.10584E-06	0.011140803	0.000136978	7.31735E-07
L16	0.10529	0.002625	6.89063E-06	0.011085984	0.000155342	8.29838E-07
L17	0.10689	0.001591	2.53128E-06	0.011425472	5.53807E-05	2.95843E-07
L18	0.10929	0.001586	2.5154E-06	0.011944304	5.26429E-05	2.81218E-07
L19	0.11078	0.001917	3.67489E-06	0.012272208	7.48508E-05	3.99853E-07
L20	0.11075	0.001687	2.84597E-06	0.012265563	5.80006E-05	3.09839E-07

L21	0.1105	0.00157	2.4649E-06	0.01221025	5.04628E-05	2.69572E-07
L22	0.10997	0.001507	2.27105E-06	0.012093401	4.69437E-05	2.50773E-07
L23	0.10962	0.001454	2.11412E-06	0.012016544	4.39796E-05	2.34939E-07
L24	0.10874	0.001595	2.54403E-06	0.011824388	5.37819E-05	2.87303E-07
L25	0.10824	0.00174	3.0276E-06	0.011715898	6.45962E-05	3.45073E-07
L26	0.10772	0.001679	2.81904E-06	0.011603598	6.0729E-05	3.24414E-07
L27	0.10733	0.00181	3.2761E-06	0.011519729	7.10875E-05	3.79749E-07
L28	0.10648	0.001701	2.8934E-06	0.01133799	6.37907E-05	3.4077E-07
L29	0.10511	0.001595	2.54403E-06	0.011048112	5.75603E-05	3.07487E-07
L30	0.10548	0.001521	2.31344E-06	0.01112603	5.19772E-05	2.77662E-07
L31	0.10556	0.001436	2.0621E-06	0.011142914	4.62605E-05	2.47123E-07
L32	0.10577	0.002785	7.75623E-06	0.011187293	0.000173267	9.2559E-07
L33	0.10584	0.004352	1.89399E-05	0.011202106	0.000422329	2.25608E-06
L34	0.1063	0.001434	2.05636E-06	0.01129969	4.54917E-05	2.43017E-07
L35	0.10266	0.002056	4.22714E-06	0.010539076	0.000100253	5.35551E-07
L36	0.10435	0.001891	3.57588E-06	0.010888923	8.20856E-05	4.38501E-07
L38	0.10375	0.001892	3.57966E-06	0.010764063	8.31254E-05	4.44056E-07
L40	0.10564	0.001817	3.30149E-06	0.01115981	7.39484E-05	3.95032E-07
L41	0.10499	0.000141	1.9881E-08	0.0110229	4.50902E-07	2.40872E-09
L42	0.10418	0.001684	2.83586E-06	0.010853472	6.53129E-05	3.48901E-07
L43	0.10498	0.000264	6.9696E-08	0.0110208	1.58101E-06	8.44573E-09
L44	0.10492	0.00202	4.0804E-06	0.011008206	9.26501E-05	4.94937E-07
L45	0.1077	0.002019	4.07636E-06	0.01159929	8.78426E-05	4.69255E-07
L46	0.11081	0.001505	2.26503E-06	0.012278856	4.61121E-05	2.46331E-07
L47	0.11019	0.001452	2.1083E-06	0.012141836	4.34061E-05	2.31876E-07
L48	0.10761	0.002928	8.57318E-06	0.011579912	0.000185019	9.88371E-07
L49	0.10365	0.001779	3.16484E-06	0.010743323	7.36359E-05	3.93363E-07
L50	0.10446	0.001612	2.59854E-06	0.010911892	5.95276E-05	3.17996E-07
L51	0.10447	0.00169	2.8561E-06	0.010913981	6.54144E-05	3.49444E-07
L52	0.10794	0.001886	3.557E-06	0.011651044	7.63119E-05	4.07658E-07
L53	0.10783	0.001541	2.37468E-06	0.011627309	5.10531E-05	2.72725E-07
L54	0.10783	0.001541	2.37468E-06	0.011627309	5.10531E-05	2.72725E-07
L55	0.10746	0.001438	2.06784E-06	0.011547652	4.47636E-05	2.39127E-07
L56	0.10609	0.00178	3.1684E-06	0.011255088	7.03672E-05	3.75901E-07
L57	0.10345	0.001464	2.1433E-06	0.010701903	5.00631E-05	2.67437E-07
L58	0.10384	0.001815	3.29423E-06	0.010782746	7.63656E-05	4.07945E-07
L59	0.10321	0.001301	1.6926E-06	0.010652304	3.97207E-05	2.12188E-07
L60	0.10175	0.001558	2.42736E-06	0.010353063	5.86078E-05	3.13083E-07
L61	0.10018	0.00155	2.4025E-06	0.010036032	5.98397E-05	3.19664E-07
L62	0.09975	0.001799	3.2364E-06	0.009950063	8.13029E-05	4.3432E-07
L63	0.09873	0.001471	2.16384E-06	0.009747613	5.54905E-05	2.9643E-07
L64	0.09781	0.001616	2.61146E-06	0.009566796	6.82334E-05	3.64503E-07
L65	0.09628	0.001389	1.92932E-06	0.009269838	5.20268E-05	2.77927E-07
L66	0.09567	0.001339	1.79292E-06	0.009152749	4.89674E-05	2.61584E-07
L67	0.09452	0.00138	1.9044E-06	0.00893403	5.32849E-05	2.84648E-07
L68	0.09329	0.001363	1.85777E-06	0.008703024	5.33599E-05	2.85049E-07
L69	0.09228	0.001453	2.11121E-06	0.008515598	6.1973E-05	3.3106E-07

Laser Beam Intensity Measurement To Derive Atmospheric Parameters

L70	0.09076	0.001548	2.3963E-06	0.008237378	7.2716E-05	3.88449E-07
L71	0.08938	0.00153	2.3409E-06	0.007988784	7.32451E-05	3.91275E-07
L72	0.08863	0.01428	0.000203918	0.007855277	0.006407048	3.42264E-05
L73	0.08709	0.001307	1.70825E-06	0.007584668	5.62997E-05	3.00753E-07

H	D	X	D^{7/3}	X⁻³	Avg
5m	0.0015	0.06	2.57561E-07	4629.62963	8.72484E-07

TABLE 5.4: Building to Building

CHAPTER - 6

CONCLUSION & FUTURE SCOPE

In conclusion, our investigation into atmospheric parameters using a scintillometer has provided valuable insights into the behavior of turbulence under various environmental conditions. Through a meticulously designed experiment comprising four distinct phases, we estimated the dynamics of atmospheric turbulence and its implications for optical communication and precision agriculture. Our analysis, encompassing data collection, derivation of the refractive index structure parameter (C_n^2) and subsequent interpretation, has contributed to the growing knowledge in the atmospheric science field.

The experimental setup, involving measurements conducted at different distances and environmental contexts, allowed us to capture the nuances of turbulence across varying scales. From room to room settings to larger-scale distances between buildings, we observed notable differences in the measured values of C_n^2 , reflecting the impact of factors such as temperature, heat flux, and surface characteristics on atmospheric turbulence.

Interpreting the results, we observed significant correlations between C_n^2 values and experimental parameters such as distance, temperature, and environmental factors. Higher C_n^2 values were often associated with increased turbulence, leading to greater signal fluctuations and beam spreading, which can degrade the performance of optical systems. Conversely, lower C_n^2 values indicated relatively calmer atmospheric conditions conducive to stable laser transmission. This nuanced understanding of turbulence behavior facilitates informed decision-making in the design and optimization of optical communication and remote sensing systems. In summary, our project represents a significant contribution to the field of atmospheric optics, offering valuable insights into the behavior of turbulence and its implications for optical systems.

The limitation of this simplified scintillometer is understood as the receive aperture of the photodetector is smaller than the laser beam aperture, after the beam propagation of 60-m in the receiver lab, where photodetector and oscilloscope DAQ are present. This limitation can be overcome by appropriate optics both at transmit and receive end of the test set up, in the future development activities.

The commercial scintillometer is envisaged and low cost modules of LEDs, Photo diodes and optics are being explored to develop scintillometers for about 100-500 meter range of field, where the majority agriculture fields in India are within this range.

CHAPTER - 7

APPLICATIONS

1. Atmospheric Research: Scintillometers are extensively used in atmospheric research to study boundary layer turbulence, air quality, and dispersion of pollutants. By measuring the fluctuations in light intensity over long paths, researchers can infer the structure and characteristics of the atmospheric boundary layer.

2. Micrometeorology: In micrometeorology, scintillometers are employed to estimate parameters like sensible heat flux, friction velocity, and the flux of pollutants. By analyzing the scintillation pattern of a laser beam across a known path, scientists can derive these micrometeorological parameters, which are crucial for understanding local weather patterns and air quality.

3. Remote Sensing: Scintillometers are utilized in remote sensing applications, particularly for monitoring atmospheric conditions over large areas. They can provide valuable data for weather forecasting, climate studies, and environmental monitoring.

4. Agriculture: Scintillometers are increasingly being used in agriculture for monitoring evapotranspiration rates, which is crucial for efficient irrigation management. By measuring the fluctuations in the laser beam caused by water vapor, researchers can estimate the rate of water loss from vegetation and soil surfaces, helping farmers optimize their irrigation practices.

5. Wind Energy: Scintillometers play a role in wind energy applications by providing information on atmospheric turbulence and wind profiles. This data is essential for optimizing the placement and operation of wind turbines to maximize energy production and ensure their structural integrity.

6. Air Traffic Management: Scintillometers can aid in air traffic management by providing real-time data on atmospheric turbulence along flight paths. Pilots and air traffic controllers can use this information to anticipate and mitigate turbulence, enhancing flight safety and passenger comfort.

7. Environmental Monitoring: Scintillometers are used in environmental monitoring programs to assess air quality, particularly in urban areas where pollution levels can vary significantly. By measuring the dispersion of pollutants in the atmosphere, scintillometers help identify sources of pollution and evaluate the effectiveness of pollution control measures.

8. Military Applications: Scintillometers in military settings aid surveillance, target identification, and optical communication assessment. They contribute to strategic planning by analyzing atmospheric conditions for aerial operations. Moreover,

scintillometer data assists in precision targeting systems despite atmospheric turbulence. Overall, their role encompasses enhancing situational awareness and optimizing military operational effectiveness.

CHAPTER - 8

BIBLIOGRAPHY

1. Springer Handbook of Atmospheric Measurements -Thomas Foken (Editor)
2. Wave Propagation in A Turbulent Medium (1961) -V. I. Tatarski
3. "The local structure of turbulence in incompressible viscous fluid for very large Reynolds numbers".- Kolmogorov, Andrey Nikolaevich (1941).
4. Study of Laser Scintillation in Different Atmospheric Conditions - P. Ernest Raj, S. Sharma, P. C. S. Devara, and G. Pandithurai.
5. A Survey of Clear-Air Propagation Effects Relevant to Optical Communications, ROBERT S. LAWRENCE AND JOHN W. STROHBEHN, MEMBER, IEEE, PROCEEDINGS OF THE IEEE, VOL. 58, NO. 10, (1970).
6. The Refractive Index Structure Parameter/Atmospheric Optical Turbulence Model: CN2 by Arnold D. Tunick. (1998).
7. Scintillometers FrankBeyrich, OscarK.Hartogensis, HenkA.R.deBruin, Helen C.Ward.
8. A new type of lidar for atmospheric optical turbulence G. G. Gimmestad, D. W. Roberts, J. M. Stewart, and J. W. Wood.
9. Engineering and Technical Solutions When Designing a Turbulent Lidar I. A. Razenkov*.
10. A lidar for remote sensing of optical turbulence W. R. Dagle, M. S. Belen'kii, G. G. Gimmestad, D. W. Roberts, and J. M. Stewart.